The Alzheimer's disease gene *SORL1* regulates lysosome function in human microglia

Swati Mishra[1,2], Nader Morshed[3,4], Chizuru Kinoshita[1,2], Beth Stevens[3,4,5], Suman Jayadev[2,6], and Jessica E. Young[1,2*]

1 Department of Laboratory Medicine and Pathology, University of Washington, Seattle, WA

2 Institute of Stem Cell and Regenerative Medicine, University of Washington, Seattle, WA

3 Boston Children's Hospital, F.M. Kirby Neurobiology Center, Boston, MA, USA

4 Stanley Center for Psychiatric Research, Broad Institute of MIT and Harvard, Cambridge, MA, USA

5 Howard Hughes Medical Institute, Boston, MA, USA

6 Department of Neurology, University of Washington, Seattle, WA

***Correspondence**

jeyoung@uw.edu

Running Title: *SORL1* and lysosome dysfunction in microglia

Acknowledgments: We acknowledge members of the Young and Jayadev laboratories for helpful critiques and discussions of this work. We also acknowledge Dr. Anna Kane in the Stevens lab for critical reading and editing of the manuscript.

Data Availability: The data that support the findings of this study are available from the corresponding author upon reasonable request.

Funding information: This study was supported by NIA R01 AG062148, R01 AG AG080585 and an Alzheimer's Association Grant 23AARG-1022491to JEY, a Development Award to SM from the UW ADRC P30 AG066509, Alzheimer's Association "Endolysosomal Defects and Neuron-glia Crosstalk in Neurodegenerative Diseases" grant to BS, and NIH training grants 5T32AG222-30 and 1F32AG079666-01 to NM.

Author Contributions: Conceptualization: SM, JEY, SJ; Experimental Methodology: SM, NM; Writing, original draft: SM, JEY; Writing, reviewing and editing: NM, BS, SJ; Funding acquisition: SM, NM, BS, JEY

KEYWORDS

SORL1, Alzheimer's disease, lysosomes, hiPSC-derived microglia, phagocytosis

Abstract

The *SORL1* gene encodes the sortilin related receptor protein SORLA, a sorting receptor that regulates endo-lysosomal trafficking of various substrates. Loss of function variants in *SORL1* are causative for Alzheimer's disease (AD) and decreased expression of SORLA has been repeatedly observed in human AD brains. *SORL1* is highly expressed by microglia, the tissue resident immune cells of the brain. Loss of SORLA leads to enlarged lysosomes in hiPSC-derived microglia like cells (hMGLs). However, whether SORLA deficiency contributes to microglia dysfunction and how this is relevant to AD is not known. In this study, we show that loss of SORLA results in decreased lysosomal degradation and lysosomal enzyme activity due to altered trafficking of lysosomal enzymes in hMGLs. Furthermore, lysosomal exocytosis, an important process involved in immune responses and cellular signaling, is also impaired in *SORL1* deficient microglia. Phagocytic uptake of fibrillar amyloid beta 1-42 and synaptosomes is increased in SORLA deficient hMGLs, but due to reduced lysosomal degradation, these substrates aberrantly accumulate in lysosomes. Overall, these data highlight the microglial endo-lysosomal network as a potential novel pathway through which *SORL1* may increase AD risk and contribute to development of AD. Additionally, our findings may inform development of novel lysosome and microglia associated drug targets for AD.

1 INTRODUCTION

Alzheimer's disease (AD), a neurodegenerative disorder and the most common cause of dementia ("2023 Alzheimer's disease facts and figures," 2023), is currently incurable. Pathological hallmarks of AD include extracellular Amyloid-beta (Aβ) plaque deposition and intracellular aggregation of tau protein known as neurofibrillary tangles. Microglia, tissue-resident phagocytes of the brain, are key effectors of pathogenic protein clearance and maintaining neuronal health and brain homeostasis in general, positioning this brain cell type at the center of cellular responses in AD

pathogenesis and making it an attractive target for AD therapy. Identification of AD risk genes highly expressed in microglia by GWAS studies further supports the idea that dysfunctional microglia may contribute to onset and/or progression of AD(Maninger et al., 2024; McQuade & Blurton-Jones, 2019). Collective evidence from murine models and post-mortem human AD brain tissue has revealed that microglia migrate to and cluster around Aβ plaques(Akiyama et al., 1999; Bolmont et al., 2008; Itagaki et al., 1989; Meyer-Luehmann et al., 2008; Stalder et al., 1999) but are unable to eliminate these toxic deposits from the brain. One mechanism that may cause this defect is lysosome dysfunction in microglia. Abnormal lysosomes in microglia can negatively alter phagocytic and inflammatory responses (Iyer et al., 2022; Lancaster et al., 2021; Joseph D. Quick et al., 2023; Ren et al., 2022), functions known to be defective in AD, substantiating the need to investigate microglia-specific lysosomal pathways as therapeutic targets. Our previous work has shown that loss of the intracellular sorting receptor and potent AD risk gene, Sortilin-related receptor-1 (*SORL1*), that encodes the multidomain protein SORLA, results in enlarged lysosomes in hiPSC-derived microglia (Mishra et al., 2024).

SORLA is a hybrid receptor that belongs to both the LDLR and the VPS10p receptor family. It interacts with the multi-protein assembly retromer and shuttles proteins between TGN, endosomes and cell surface (Fjorback et al., 2012; Jacobsen et al., 2001; Jacobsen et al., 1996; Willnow & Andersen, 2013; Yamazaki et al., 1996). Studies have also shown that SORLA can traffic Aβ peptides to lysosomes (Caglayan et al., 2014). Genetic, epidemiological and functional studies have now cumulatively and unequivocally established *SORL1* as a gene that increases risk for AD. (Holstege et al., 2017; Holstege et al., 2023; Kunkle et al., 2017; Lambert et al., 2013; Rogaeva et al., 2007; Scheltens et al., 2021). Loss of SORLA expression has been observed in AD brains from early stages of the disorder (Dodson et al., 2006; Scherzer et al., 2004; Thonberg et al., 2017). Studies investigating the role of SORLA in AD pathogenesis have extensively focused on neurons and revealed that loss of SORLA causes defects in the endo-lysosomal pathway of hiPSC-derived neurons, specifically in endosomal recycling, autophagy and lysosome function, ultimately resulting in increased secretion of toxic Aβ species and impaired synaptic activity in neurons(Andersen et al., 2022; Hung et al., 2021; Knupp et al., 2020; Lee et al., 2023; Mishra et al., 2023; Mishra et al., 2022). While *SORL1* mRNA is highly expressed in microglia, even more so than neurons and astrocytes(Lee et al., 2023; Olah et al., 2018; Zhang et al., 2016), the impact of loss of SORLA function specifically in microglia is not well-studied, rendering our

understanding of the role of SORLA in AD risk incomplete at best. Understanding cell type specific functions of AD risk genes, including SORLA, is imperative to understand the etiology and pathogenesis of the disease, and to develop rational therapeutic approaches for AD.

In this study, we investigated the role of SORLA in regulating lysosome function in hiPSC-derived microglia like cells (hMGLs). We used quantitative flow cytometry, immunocytochemistry, and functional enzymatic and cellular assays to reveal that *SORL1* KO hMGLs show decreased lysosomal degradation and reduced lysosomal enzymatic activity, possibly due to reduced trafficking of lysosomal enzymes from the trans-Golgi network (TGN) to lysosomes. We also provide evidence that altered lysosomal exocytosis, a secretory pathway through which microglia release lysosomal enzymes and inflammatory cytokines into the extracellular environment, is one mechanism contributing to lysosomal abnormalities in *SORL1* KO hMGLs. We find that depletion of *SORL1* causes accumulation of intracellular fibrillar Aβ 1-42 and synaptosomes because of both increased phagocytic uptake and reduced lysosomal degradation. Finally, we show that *SORL1* KO hMGLs have a reduced inflammatory response. Overall, our data show that *SORL1* regulates lysosomal homeostasis in human microglia. Loss of normal *SORL1* function leads to mis-trafficking of lysosomal enzymes and impairment of critical lysosomal functions, including lysosomal exocytosis. This data contributes to a growing body of work highlighting *SORL1* and related pathways as novel therapeutic targets for AD.

2. MATERIALS AND METHODS

2.1 Differentiation of human iPSCs into microglia like cells (hMGLs)

hiPSCs were differentiated into hMGLs as previously described with some modifications (McQuade et al., 2018). Briefly, hiPSCs were plated in mTESR plus medium supplemented with ROCK Inhibitor (Y-27632; # A3008 ; Apex Bio) on Matrigel (Growth factor reduced basement membrane matrix; # 356231; Corning) coated 6 well plates (#657160; CELLSTAR). To begin hematopoietic progenitor differentiation, these cells were passaged to get a density of ~10 colonies per well of a 6 well plate. On day 0, mTESR plus medium was replaced with STEMdiff™ Hematopoietic Supplement A medium from the STEMdiff™ Hematopoietic kit (# 05310; STEMCELL technologies). On day 3, when colonies became flattened, medium was replaced with STEMdiff™ Hematopoietic Supplement B medium from the STEMdiff™ Hematopoietic kit (# 05310; STEMCELL technologies). Cells remained in this medium for 7 additional days. By day

12, non-adherent hematopoietic progenitor cells (HPCs) coming off from the flattened colonies were harvested by removing medium. Any remaining HPCs/floating cells were collected by gentle PBS washes. At this point, HPCs were either frozen using Bambanker cell freezing medium (#BBH01; Bulldog-Bio) or plated at a density of 0.2 million cells per well of a Matrigel coated 6 well plate in microglia differentiation medium for 24 days. Microglia differentiation medium comprised of DMEM-F12 (#11039047; Thermo Fisher Scientific) , Insulin-transferrin-selenite (#41400045; Thermo Fisher Scientific), B27 (# 17504-044; Thermo Fisher Scientific), N2 (# 17502-048; Thermo Fisher Scientific), Glutamax (# 35050061; Thermo Fisher Scientific) , non-essential amino acids (# 11140050; Thermo Fisher Scientific), monothioglycerol (# M1753; Sigma), Insulin (# I2643; Sigma) freshly supplemented with TGF-β (#130-108-969, Miltenyi), IL-34 (# 200-34; Peprotech) and M-CSF (#PHC9501; Thermo Fisher Scientific). On day 24, this medium was supplemented with CD200 (#C311; Novoprotein) and CX3CL1 (#300-31; Peprotech) for maturation of microglia. Cells remained in this medium for 8 days. On day 32, microglia differentiation was complete, and these cells were plated on Poly-l-lysine (#P6282; Sigma; 100µg/ml) coated coverslips (12mm diameter, #1760-012; cglifesciences) in a 24 well plate for immunocytochemistry with appropriate antibodies or Poly-l-lysine coated 48 well plates for flow cytometry.

2.2 Meso-Scale Discovery (MSD) V-PLEX platform to measure extracellular levels of cytokines in hMGLs

Pro-inflammatory cytokines in the media were measured using the Proinflammatory Panel 1 (human) kit (#K15049D; MSD V-PLEX MULTI-SPOT assay System; MesoScale Diagnostics). For this assay, hMGLs were plated at a density of 100,000 cells/well of a matrigel coated 96 well plate and allowed to settle for 24 hours. Cells were then treated with 20 ng/ml IFNγ or 100ng/ml Lipopolysaccharide (LPS) for 24 hours. Conditioned media was harvested at the end of 24 hours and stored at -80°C until use. 50µl of media was used to run the MSD V-plex assay as per manufacturer's protocol and MSD Quick plex SQ120 instrument was used to detect analytes. This MSD V-Plex Proinflammatory Panel detects a panel of Pro-inflammatory cytokines including IL-1β, IL-6, IL-8, IFN-γ, TNF-α, IL-13, IL-2, IL-4, IL-10 and IL-12p70, known to be altered in AD patients (Park et al., 2020; Taipa et al., 2019).

2.3 In vitro fibrillation of Amyloid-β (1-42) (fAβ)

HiLyte Fluor 647 beta-amyloid (1-42) (# AS-64161, Anaspec) was fibrillized as described previously (Amos et al., 2017). Briefly, Aβ-42 was resuspended in sterile 1X PBS to generate a final concentration of 100µM, placed at 37°C for 5 days for fibrillization, aliquoted and stored at -80°C.

2.4 Phagocytosis of fibrillar Amyloid-β (1-42)

To measure phagocytosis of fAβ by hMGLs, Aβ labeled with a fluorophore, HiLyte Fluor 647 beta-amyloid (1-42) (# AS-64161, Anaspec) was fibrillized as described above. hMGLs were plated at a density of 100,000 cells per well of a Poly-l-lysine (100µg/ml) coated 48 well plate. Cells were treated with this fAβ (0.1µM) for 30 mins, 5 hours and 24 hours. At the end of each time point, cells were washed with 1X PBS and harvested using accutase. Intracellular fluorescence of fAβ was measured using flow cytometry. Data was analyzed using Flow Jo software. Fluorescence measured at 30 mins indicates uptake efficiency and the longer time points can either indicate sustained phagocytic capacity of hMGLs or accumulation of undegraded substrates in the lysosomes. As an additional method to test phagocytosis of fibrillar Aβ by hMGLs, phagocytosis assay was performed as described above. Subsequently, phagocytosis was examined using immunocytochemistry with cells fixed with 4 % PFA in PBS for 10 mins and imaged using the Leica SP8 microscope.

2.5 Phagocytosis of synaptosomes

To measure phagocytosis of synaptosomes, a phagocytosis assay was performed as previously described with some modifications(Beeken et al., 2022). Briefly, synaptosomes were harvested from Wildtype hiPSC-derived neurons using Syn-PER Synaptic Protein Extraction Reagent (# 87793; Thermo Fisher Scientific). 3 ml Syn-PER reagent was added to 1 10cm cell culture plate of neurons (~30M cells), cells were harvested by scraping and centrifuged at 1200g for 10 mins. The supernatant was collected and centrifuged at 15,000g for 20 mins at 4ºC and the pellet which are the synaptosomes (crude synaptosome extraction) were either resuspended in Krebs ringer solution (with 1X protease inhibitor) and frozen at -80°C or labeled with CM-Dil cell tracker dye (final concentration 3µM) as per manufacturer's instructions (#C7000; Thermo Fisher Scientific). CM-Dil labeled synaptosomes were added to hMGLs plated on Poly-l-lysine coated 48 well plates and cells were harvested at the end of different time points including 30 mins, 5 hours, and 24 hours. The intracellular fluorescence intensity of CM-Dil labeled synaptosomes was measured

using flow cytometry as a readout of phagocytosis of synaptosomes by hMGLs. To further confirm phagocytosis of synaptosomes by hMGLs, phagocytosis assay was performed as described above followed by immunocytochemistry with cells fixed with 4 % PFA in PBS for 10 mins and imaged using the Leica SP8 microscope.

2.6 Western blotting

For western blot analysis, cell lysates were harvested from hMGLs using RIPA protein lysis buffer (#20-188; Millipore) containing 1X protease and 1X phosphatase inhibitors (#PI78443; ThermoFisherScientific). Total protein concentration was quantified using Pierce BCA assay kit (#23225; Thermo Fisher Scientific). 10-20µg of protein lysates were run on 4%–20% Mini-PROTEAN TGX Precast Protein Gels (#4561096; Biorad) and transferred to PVDF membranes. Membranes were blocked with 5% w/v non-fat dry milk in 1X PBS (blocking buffer), washed with 1X PBS with 0.05% tween 20 (PBST) and incubated overnight at 4ºC with the following primary antibodies diluted in 0.2% sodium azide+5% BSA in 1X PBS : Sortilin-related receptor 1 (SORLA) at 1:1000 (# ab190684; abcam); Mouse monoclonal anti-Actin (clone A4) (#MAB1501; Millipore Sigma) at 1:2000; Rabbit monoclonal anti-HEXB (#ab140649; abcam); Goat anti-Cathepsin B (#ab214428; abcam); Mouse monoclonal anti-Cathepsin D (#ab6313; abcam) and Rabbit monoclonal anti-LAMP1 (#9091S; Cell signaling). Membranes were then washed with PBST, incubated in corresponding HRP conjugated secondary antibodies for 1h. The following secondary antibodies were used. Goat anti-Mouse IgG (H+L) Secondary Antibody HRP (#31430; Thermofisher Scientific) Goat anti-Rabbit IgG (H+L) Secondary Antibody HRP (# 31460; Thermofisher Scientific) and Donkey anti-goat IgG (H+L) Secondary Antibody (#A15999; ThermoFisher Scientific). Membranes were then washed thrice with PBST, probed with either Clarity Western ECL substrate (#1705061; Biorad) or Clarity Max Western ECL Substrate and scanned using an Odyssey Clx imaging system (Li-Cor) to detect bound proteins on membranes.

2.7 Lysosomal degradation assay

Lysosomal degradation in hMGLs was measured using DQ-BSA (#12051; Thermo Fisher Scientific) which is a fluorogenic substrate for proteases and fluoresces only when degraded in lysosomes. For this assay, hMGLs were plated at a density of 100,000 cells per well of a Poly-l-lysine coated 48 well plate. A pulse-chase experiment was performed wherein hMGLs were treated with 20µg/ml DQ-BSA for 20 mins. At the end of this timepoint, cells were washed with 1X PBS

and cultured in complete microglia medium for 30 mins, 2 hours, and 5 hours. At the end of each timepoint, cells were washed with 1X PBS and harvested using accutase. Intracellular fluorescence intensity of DQ-BSA was measured using flow cytometry and data was analyzed using flow jo software. Altered fluorescent intensity of DQ-BSA was measured as a readout of altered lysosomal degradation. As an additional method to examine lysosomal degradation, we performed pulse chase experiment as described above and immunocytochemistry (cells fixed after 2h) after treating cells with DQ-BSA and intracellular fluorescence intensity was noted as a readout of lysosomal degradation. Treatment with the lysosomotropic agent chloroquine (50µM) was used as a negative control for both experiments.

2.8 Lysosomal enzyme activity assays

To measure lysosomal enzyme function, lysosomal enzyme activity assays were performed. For hMGLs generated using protocol based on McQuade et al 2018, 200,000 hMGLs were plated per well of a poly-l-lysine coated 48 well plate. Cells were allowed to settle for 24 hours. Specifically, enzyme activity of lysosomal enzymes, Cathepsin D (#ab65302; abcam), Cathepsin B (#ab 65300; abcam) and Hexosaminidase B (#MET-5095; Cell Bio labs) was measured as per manufacturers protocol.

2.9 Colocalization analysis

To investigate colocalization of lysosomal enzymes with the TGN or lysosomes, hMGLs were plated in a 24 well plate with 12mm diameter coverslips, allowed to settle for 48 hours and fixed with 4% PFA in PBS. Immunocytochemistry was performed using primary antibodies against lysosomal enzymes, Cathepsin B, Cathepsin D and HEXB and TGN marker, TGN38 and late endosomal and lysosomal marker, LAMP1. Cells were co-labelled for either TGN and lysosomal enzymes or LAMP1 and lysosomal enzymes. For the lysosomal enzymes, the same antibodies were used for both immunocytochemistry and western blotting. To label TGN and lysosomes, TGN38 (B6) mouse monoclonal antibody (#166594; SantaCruz) and LAMP1 mouse monoclonal antibody (#sc20011; Santacruz) were used. A minimum of 10 fields of confocal images were captured using the Leica SP8 microscope. Images were analyzed using Image J software. Median filtering was used to remove noise from images and Otsu thresholding was applied to all images. Colocalization was quantified using the JACOP plugin in ImageJ software and presented as Mander's correlation coefficient.

2.10 Confocal microscopy and image processing

All microscopy and image processing were performed under blind conditions. Z stack images were acquired using the Leica TCS SP8 confocal laser microscope with 63x/1.40 oil lens (Leica Microsystems) and modified/processed using Leica Application Suite X 3.5.5.19976 with LIGHTNING adaptive deconvolution (Leica Microsystems). 10-20 fields were imaged per experiment per clone, which included a total of 50-100 cells. For some experiments, images were processed further using Image J software (Schindelin et al., 2012).

2.11 Measurement of surface LAMP1 expression

To measure surface LAMP1 expression, hMGLs were plated at a density of 100,000 cells per well of a 48 well plate and allowed to settle for 48 hours. Cells were then either treated with the calcium ionophore, calcimycin (#C4403; Sigma) +4mM $CaCl_2$+0.1% BSA in PBS to stimulate LE or 0.1%BSA in PBS as control and placed in the cell culture incubator for 30 mins. Next, cells were placed on ice for 15 mins and treated with cold Mouse monoclonal antibody against LAMP1(#328611; Biolegend) specific to the N terminal luminal epitope of the antigen, for an hour on ice. Cells were then washed with 1X PBS and either treated with accutase and used for flow cytometry or fixed with 4% PFA in PBS for 5 mins and used for immunocytochemistry. Surface expression of LAMP1 was presented as fluorescence measured by flow cytometry and Flow Jo software or immunocytochemistry and Image J software.

2.12 Quantification and statistical analysis

All data presented in this study represent multiple hiPSC clones. This includes two clones for WT hMGLs and two clones for *SORL1* KO hMGLs. All data represent at least six independent experiments (called replicates) per clone. Experimental data were tested for normal distributions using the Shapiro-Wilk normality test. Normally distributed data were analyzed using parametric two-tailed unpaired t tests, one-way ANOVA tests, or two-way ANOVA tests. Significance was defined as a value of $p < 0.05$. All statistical analysis was completed using GraphPad Prism software.

3 Results

3.1 Loss of *SORL1* decreases lysosomal degradation in hMGLs

We have previously shown that *SORL1* KO hMGLs have enlarged lysosomes indicating lysosome dysfunction and stress(Mishra, 2024). We next asked if *SORL1* KO hMGLs show altered lysosomal degradation. We generated WT and *SORL1* KO hematopoietic progenitor cells (HPCs) and hMGLs using a previously published protocol with minor modifications(McQuade et al., 2018). HPC-specific expression was confirmed in WT and *SORL1* KO HPCs using immunostaining with the HPC marker CD43 and microglia specific expression was demonstrated by immunostaining with the microglia markers IBA1, CX3CR1, P2RY12 and TMEM119. Loss of *SORL1* did not alter differentiation of hiPSCs into HPCs and hMGLs (Figure S1). To determine if overall proteolytic lysosomal degradation is affected, we performed a pulse chase assay with DQ-Red-BSA, a fluorogenic substrate that fluoresces only upon degradation (Marwaha & Sharma, 2017) (Figure 1A). Mean fluorescence intensity (MFI) was measured by flow cytometry as a readout of lysosomal degradation. Both WT and *SORL1* KO hMGLs showed an increase in MFI over a period of 2h suggesting our hiPSC-derived microglia were capable of lysosomal degradation *in vitro*, although *SORL1* KO hMGLs demonstrated reduced MFI of DQ-Red-BSA as compared to WT hMGLs at all time points tested (Figure 1B), suggesting either decreased uptake and/or degradation of the substrate. Uptake of DQ-Red-BSA occurs through pinocytosis(Reis et al., 1998) and short-term uptake of this substrate cannot be measured because it fluoresces only upon reaching lysosomes. Therefore, we tested uptake of a proxy reagent, BSA conjugated to a red fluorophore (BSA-594), which also undergoes pinocytic uptake. Inhibiting lysosome proteolysis by the lysosomotropic reagent chloroquine abrogated lysosomal degradation of DQ-BSA in both WT and *SORL1* KO hMGLs (Figure 1B, D-E), validating our degradation assays. Interestingly, we observed an increased uptake of BSA-594 in *SORL1* KO hMGLs as compared to WT hMGLs (Figure 1C). Together, this data suggests that *SORL1* KO hMGLs have reduced lysosomal degradation of DQ-BSA rather than reduced uptake of substrates. To further confirm our findings with an independent method, we performed a pulse chase assay and immunocytochemistry. Specifically, we incubated hMGLs with DQ-Red-BSA similar to the experiment described above and cells were fixed after 2 hours. Immunocytochemistry was performed to label cells with the microglia marker CX3CR1. In accordance with our hypothesis, we observed decreased lysosomal degradation in *SORL1* KO hMGLs as compared to WT hMGLs (Figure 1D, E). Overall, our data demonstrated that loss of *SORL1* causes decreased lysosomal degradation in hMGLs.

3.2 Loss of *SORL1* decreases intracellular lysosomal enzyme activity in hMGLs.

Next, we investigated intracellular lysosomal enzyme activity as a potential cause for altered lysosomal degradation observed in *SORL1* KO hMGLs. We tested intracellular enzyme activity of three key lysosomal enzymes, Beta-hexosaminidase subunit beta (HEXB), Cathepsin D (CTSD) and Cathepsin B (CTSB). All three enzymes are highly expressed in microglia, CTSD and CTSB have been proposed to degrade Aβ and tau, and altered expression of all three enzymes has been observed in AD(Cermak et al., 2016; Di Spiezio et al., 2021; Hamazaki, 1996; Ii et al., 1993; Kenessey et al., 1997; Kuil et al., 2019; Sierksma et al., 2020; Sun et al., 2008; Whyte et al., 2022). Furthermore, altered expression or activity of these enzymes causes significant lysosome dysfunction and affects Aβ deposition in mouse brains (Keilani et al., 2012; Koike et al., 2000; Oberstein et al., 2021; Suire et al., 2020; Suzuki et al., 2022; Wang et al., 2012). Depletion of *SORL1* resulted in reduced lysosomal enzyme activity of HEXB, CTSD and CTSB (Figure 2A-C) without altering protein expression in *SORL1* KO hMGLs relative to WT hMGLs (Figure 2 D-F). Chloroquine treatment was used as a negative control in enzyme activity assays and as expected, resulted in decreased lysosomal enzyme activity for all the enzymes (Figure 2A-C). To further confirm our hypothesis and account for potential heterogeneity introduced by microglia differentiation protocols, we tested lysosomal enzyme activity in iPSC-derived microglia generated using a different protocol (Dolan et al., 2023). Characterization of these hMGLs showed no difference in expression of microglia-specific markers between WT and *SORL1* KO cells (Figure S2A). Using these hMGLs, we independently confirmed reduction in intracellular CTSD activity (Figure S2B), validating our hypothesis that loss of *SORL1* results in reduced lysosomal enzyme activity. Overall, our data suggests that decreased lysosomal enzyme activity, rather than changes in lysosomal protein expression, contributes to the differences in lysosomal degradation and enlarged lysosomes observed in *SORL1* KO hMGLs. Our results are concordant with a recent study that showed no difference in mRNA and protein expression of CTSD, CTSB and HEXB using mRNA-sequencing and TPT proteomics (Lee et al., 2023). Furthermore, lysosomal phenotypes due to *SORL1* deficiency are not due to differences between *in vitro* differentiation protocols.

3.3 Loss of *SORL1* results in altered trafficking of lysosomal enzymes in hMGLs.

Newly synthesized lysosomal enzymes are transported from the Golgi to the lysosome using either a mannose-6-phosphate (M6P)-dependent pathway primarily regulated by the multi-protein

complex retromer (Arighi et al., 2004; Thomas Braulke & Juan S. Bonifacino, 2009; Cui et al., 2019) or in a M6P-independent pathway in which enzymes are directly targeted to the lysosome(Nielsen et al., 2007). To test whether lysosomal enzymes are intracellularly mis-localized, we used immunocytochemistry with antibodies that recognized both immature and mature forms of the lysosomal enzymes Cathepsin B, Cathepsin D and HEXB. We measured colocalization of these enzymes at the TGN and the lysosomes using the TGN marker TGN38 and the late endosome and lysosome marker, LAMP1. Our results showed increased colocalization of all three enzymes with TGN38 (Figure 3A,C,E) and decreased colocalization with LAMP1 (Figure 3B,D,F) suggesting that the enzymes are not appropriately trafficked to the lysosomes from the TGN. As we observed decreased enzyme activity but no change in total protein expression of CTSD, CTSB and HEXB, our data suggested that dysfunction in lysosomal degradation is likely due to mis-trafficking of lysosomal enzymes.

3.4 Loss of *SORL1* decreases lysosomal exocytosis (LE) in hMGLs.

To further validate the role of *SORL1* in microglia lysosome function, we next investigated if the lysosome secretory pathway, lysosomal exocytosis (LE), is affected by loss of *SORL1*. LE is a calcium-dependent process that involves fusion of lysosomes with the plasma membrane, exposing the luminal domain of LAMP1 on the cell surface resulting in release of lysosomal contents into the extracellular environment (Andrews, 2000; Blott & Griffiths, 2002). Murine microglia are known to utilize LE to maintain cellular homeostasis and respond to external stimuli by releasing lysosomal enzymes and cytokines outside the cell(Andrei et al., 2004; Dou et al., 2012; Eder, 2009). However, LE has not been demonstrated in human microglia and mechanisms regulating this process are not completely understood. We hypothesized that altered LE can be a consequence of lysosome dysfunction observed in *SORL1* KO hMGLs. To investigate LE function in *SORL1* KO hMGLs, we induced LE with the ionophore calcimycin (Jaiswal et al., 2002) and labeled cells with an antibody specific to the luminal epitope of LAMP1(Andrews, 2017) to visualize surface expression of LAMP1 via flow cytometry and immunocytochemistry. Both WT and *SORL1* KO hMGLs showed an increase in surface expression of LAMP1 upon calcimycin treatment, suggesting that hMGLs can undergo LE *in vitro*. However, *SORL1* KO hMGLs exhibited reduced surface LAMP1 expression as compared to WT in both stimulated and unstimulated conditions, as evidenced by immunocytochemistry (Figure 4A) and flow cytometry (Figure 4B) showing that

loss of *SORL1* results in decreased LE in hMGLs. Because LE causes extracellular release of lysosomal enzymes, we measured extracellular lysosomal enzyme activity. We found reduced extracellular enzyme activity of HEXB, Cathepsin B and Cathepsin D in *SORL1* KO hMGLs (Figure 4C-E). This reduction in extracellular enzyme activity along with the reduction in cell surface LAMP1 expression strongly indicates that LE is impaired in *SORL1* KO hMGLs. In addition, as the extracellular release of lysosomal enzymes is a normal part of LE, often contributing to extracellular matrix remodeling or cell-cell communication (Buratta et al., 2020), the general reduction in lysosomal enzyme activity observed in *SORL1* hMGLs may further confound the LE process. To further confirm our hypothesis, we used fluorometric detection to measure extracellular lysosomal enzyme activity of HEXB and Cathepsin D as a readout of LE in a second model of hMGLs(Dolan et al., 2023). *SORL1* KO hMGLs showed decreased extracellular enzyme activity of both enzymes (Figure S2, C-D), validating the idea that loss of *SORL1* causes decreased LE in hMGLs irrespective of the method used to generate microglia from hiPSCs. Taken together, our data provide evidence of LE in human microglia *in vitro* and identify *SORL1* as a novel regulator of this lysosomal secretory process in microglia.

3.5 Loss of *SORL1* causes lysosomal accumulation of Aβ and synaptosomes in hMGLs

Given that depletion of *SORL1* causes reduced lysosomal degradation and reduced LE in hMGLs, we hypothesized that *SORL1* KO would increase lysosomal burden and cause accumulation of substrates in dysfunctional lysosomes of *SORL1* KO hMGLs. To test this idea, we measured lysosomal accumulation of fluorophore-labeled fibrillar Aβ 1-42 (fAβ) and CM-Dil dye labeled synaptosomes using pulse chase assays and immunocytochemistry. Consistent with our hypothesis, *SORL1* KO hMGLs showed increased accumulation of both substrates as evidenced by increased colocalization of Aβ 1-42 and synaptosomes with LAMP1 (Figure 5A-D). Increased phagocytosis can contribute to increased accumulation of these substrates, so we tested whether phagocytic uptake was altered in *SORL1* KO hMGLs. To analyzed uptake and sustained phagocytosis we incubated cells with fluorophore-labeled fAβ and synaptosomes for 30 mins, 5h and 24h and observed increased uptake and sustained phagocytosis of both substrates in *SORL1* KO hMGLs as compared to WT hMGLs (Figure 5 E-H). To confirm an impairment in substrate degradation, we treated cells with Aβ conjugated to the pH sensitive dye, pHrodo, performed a pulse chase assay, and measured fluorescence of Aβ-pHrodo. Our results revealed no difference in

fluorescence intensity at time 0 but decreased fluorescence intensity of pHrodo after a chase period of 30 min, 2h and 5h in *SORL1* KO hMGLs (Figure S3). Together, this data suggests that through increased phagocytic uptake combined with impaired lysosomal degradation and the reduced ability to release un-degraded substrates into the extracellular environment via LE, loss of *SORL1* ultimately causes lysosomal accumulation of substrates in hMGLs. Altogether, our data demonstrates that loss of *SORL1* significantly increases lysosomal dysfunction in human microglia.

3.6 Loss of *SORL1* results in decreased inflammatory response in hMGLs.

Aberrant lysosome function can negatively impact the neuroimmune response of microglia (J. D. Quick et al., 2023; Van Acker et al., 2021), and LE is one of the secretory pathways for cytokine secretion in immune cells (Blott & Griffiths, 2002; Semino et al., 2005) including microglia (Allendorf & Brown, 2022), suggesting that impaired LE might prevent cytokine secretion in hMGLs. Thus, we hypothesized that loss of *SORL1* will result in a blunted inflammatory response of hMGLs. We assessed levels of cytokines known to be released by LE in immune cells, including IL-1β (Figure 6A)(Andrei et al., 2004; Gardella et al., 2001; Monif et al., 2016) and IL-12p70 (Figure 6B)(Chiaruttini et al., 2016), to be reduced in *SORL1* KO MGLs, both unstimulated and stimulated with pro-inflammatory stimuli, Lipopolysaccharide (LPS) (100ng/ml) and IFNγ (20ng/ml) for 24 hours (Figure 6). Furthermore, *SORL1* KO hMGLs showed decreased extracellular secretion of pro-inflammatory cytokines IL-6, IL-15, IP-10, TNF-α and IL-8 (Figure 6C-G) and anti-inflammatory cytokines IL-10, IL-13, and IL-2 (Figure 6H-J) known to be secreted by LE-independent pathways, including regulated and constitutive exocytosis (Stanley & Lacy, 2010). Interestingly, unstimulated *SORL1* KO hMGLs demonstrated reduced extracellular levels of IL-6, IL-2p70 (IL-12), IP-10, IL-1β and IL-8 (Figure 6A-E) but no change in IL-10, IL-15, IL-13, IL-2 and TNF-α (Figure 6F-J). Although cytokine levels in unstimulated cells were very low, this data suggests that cytokine release regulated by SORLA may be context dependent. Altogether, these data reveal a novel function of SORLA in regulating inflammatory response in human microglia potentially through several cytokine secretion mechanisms including lysosomal exocytosis.

4. Discussion

Despite extensive evidence that loss of function variants in the *SORL1* gene and *SORL1* haploinsufficiency are causative for AD(Campion et al., 2019; Holstege et al., 2017; Nicolas et al., 2016; Pottier et al., 2012; Verheijen et al., 2016), developing therapeutic interventions targeting *SORL1* has been challenging, partly because cell type-specific mechanisms through which loss of *SORL1* may increase risk for AD remain unclear. Indeed, recent RNA sequencing data highlights that certain CNS cells undergo more changes than others in response to *SORL1* KO(Lee et al., 2023). Recent work from our group and others has shown that depletion of SORLA leads to enlarged early endosomes, impairments in endo-lysosomal trafficking, changes in gene expression and impaired neuronal function (Hung et al., 2021; Knupp et al., 2020; Lee et al., 2023; Mishra et al., 2023; Mishra et al., 2022). Despite this extensive characterization in neurons, very little is currently understood about SORLA function in human microglia. Our study provides evidence for the role of SORLA in regulating lysosome function in human microglia. We show that loss of SORLA causes mis-trafficking of lysosomal enzymes and impaired lysosomal homoeostasis in microglia, highlighting lysosome-associated pathways as one mechanism potentially contributing to aberrant microglial responses in early stages of AD.

4.1 SORLA and lysosomal homeostasis in human microglia

Our data collectively shows that SORLA-deficient hMGLs have reduced lysosomal degradation, enzyme activity, and altered trafficking of lysosomal enzymes from the TGN to lysosomes. SORLA binds to retromer(Fjorback et al., 2012), which regulates the retrograde transport of the cation independent mannose-6-phosphate receptor (CIMPR) through the Mannose-6-Phosphate dependent pathway (M6P) (Arighi et al., 2004; Cui et al., 2019). The CIMPR is a key receptor that traffics lysosomal enzymes from the TGN to the lysosomes (Thomas Braulke & Juan S Bonifacino, 2009; Braulke et al., 2023) In the absence of SORLA, the retromer-mediated retrograde transport of CIMPR may be impaired, leading to an accumulation of lysosomal hydrolases in the TGN. In support of this idea, it has been shown in immortalized neuroblastoma and epithelial cell lines that SORLA can bind to the cytosolic adaptor protein, phosphofurin acidic cluster sorting protein 1 (PACS1)(Burgert et al., 2013) which is known to direct retrograde TGN retrieval of CIMPR(Chen et al., 1997; Scott et al., 2006; Wan et al., 1998) and can participate in PACS1 dependent sorting of Cathepsin B(Burgert et al., 2013). SORLA has also been shown to shuttle lysosomal enzymes from the TGN to the lysosomes independent of the CIMPR pathway (Nielsen et al., 2007). Taken

together, it is reasonable to hypothesize that SORLA may regulate lysosomal targeting of enzymes through either M6P dependent or independent pathways in human microglia.

Our data supports a hypothesis that it is primarily altered TGN-lysosome trafficking that leads to the decrease in lysosomal enzyme activity. We did not observe significant differences in total protein or changes in pro vs. mature forms of lysosomal enzymes (Figure 2D-F). One explanation for this observation could be that there are different ratios of pro vs. mature forms of these enzymes in other compartments (such as endosomes) or that there is leakage of mature enzymes from the lysosome to the cytoplasm. Interestingly, proteomic analyses have shown differences in expression of lysosomal enzymes from *SORL1*-deficient microglia, in one case showing no change (Lee et al., 2023) and in another showing decreased expression although the majority of this decrease was reported from a cell line with a missense variant in the VPS10 domain of *SORL1* (Liu et al., 2020). The nuances of how alterations in SORLA expression affect lysosomal homeostasis are likely complex and future work is needed to unravel the exact mechanisms. The data in this study suggests that loss of SORLA leads to decreased activity of lysosomal enzymes. This likely impairs the degradation of Aβ and other substrates, such as excess myelin fragments, that contribute to the increased amyloidogenic burden and lipid overload observed in the early stages of AD.

4.2 SORLA and phagocytosis in human microglia

Our study reveals that, while degradation is impaired in *SORL1* KO hMGLs, loss of SORLA results in increased phagocytic uptake of substrates (Figure 5). The impact of this increased phagocytosis of synaptosomes could contribute to excessive synaptic pruning and eventual synaptic loss observed in AD, but increased uptake of fAβ may be a means to reduce amyloidogenic burden. SORLA is known to regulate receptor protein homoeostasis at the cell surface by modulating intracellular sorting of receptors to the TGN and endo-lysosomal compartments. It is possible SORLA plays a potential regulatory role in sorting of phagocytic receptors in human microglia and loss of SORLA may cause increased presence of these receptors at the cell surface, ultimately resulting in increased phagocytic uptake. In agreement with this idea, Liu et al. observed expression changes in phagocytic receptors in *SORL1* deficient hMGLs including ITGB2, a receptor involved in the phagocytosis of both Aβ and synaptosomes(Liu et al., 2020). However, in their study, Liu et al. observed deficient phagocytosis of oligomeric Aβ, although the assay did not distinguish between phagocytic uptake and substrate degradation. Mechanisms of phagocytic

uptake by microglia can also differ significantly depending on the protein conformation of Aβ(Pan et al., 2011; Ries & Sastre, 2016). Another recent study observed increased expression of the AD risk gene *BIN1* in *SORL1* KO hMGLs(Lee et al., 2023), which may lead to increased phagocytosis(Sudwarts et al., 2022). Together, this data suggests that loss of *SORL1* expression may change levels of surface phagocytic receptors and genes involved in phagocytosis.

While we observe increased phagocytic uptake of both fAβ and synaptosomes, these substrates were not degraded, therefore a crucial aspect of the normal phagocytic process in *SORL1* KO hMGLs is impaired leading to their intracellular accumulation. This may ultimately increase lysosomal stress in microglia and contribute to lysosomal dysfunction seen in AD. Indeed, the role of SORLA in microglial phagocytosis may act as a 'double-edged sword', functioning in both a disease-stage specific and context-dependent manner.

4.3 *SORL1* deficient hMGLs have impaired lysosomal exocytosis and a blunted immune response.

In this study we found that *SORL1* KO hMGLs show reduced LE as evidenced by reduced LAMP1 localization on the plasma membrane and reduced enzyme activity in the conditioned medium of hMGLs after treatment with a stimulus. Lysosomal exocytosis (LE) is a calcium-regulated process that expels lysosomal contents into the extracellular space(Buratta et al., 2020; Tancini et al., 2020). LE is important for such activities as remodeling of the extracellular matrix and, in the case of immune cells, releasing contents to degrade pathogenic material (Ireton et al., 2018; Miao et al., 2015).

Our study reveals a novel role for SORLA in regulation of microglial LE. SORLA may modulate calcium homeostasis, either via interaction with protein-interacting C Kinase 1 (PICK1) (Binkle et al., 2022), which has been shown to be a calcium sensor in mouse microglia (Zhu et al., 2016), or through regulation of palmitoyl-protein thioesterase-1 (ppt1) (Mondal et al., 2022) which is known to regulate lysosomal calcium homoeostasis. However, future work will be required to definitively elucidate the mechanism by which SORLA regulates LE.

The relationship between SORLA deficiency and LE raises compelling questions about the role of LE in AD. LE could support degradation of Aβ via release of lysosomal enzymes to the extracellular space, and LE may alleviate lysosomal stress by the extracellular release of

undegraded substrates. Interestingly, in response to an acute stress, LE can be used to release pro-inflammatory cytokines such as IL1-β and TNFα, bypassing the slower, more conventional secretory pathway (Aiello et al., 2020). Indeed, we observed that when stimulated by either LPS or IFNγ, *SORL1* KO hMGLs showed a blunted cytokine release (Figure 6). Thus, loss of *SORL1* may reduce LE at early stages of AD, leading to impaired clearance and stunted inflammatory response of microglia to accumulating pathogenic proteins in AD. Additionally, increased stress on lysosomes due to SORLA-mediated impaired degradation may lead to an increasingly pathogenic environment for microglia. Interestingly, increased levels of extracellular lysosomal proteins, including lysosomal enzymes and LAMP1, have been observed colocalized with amyloid plaques and in the CSF of AD patients (Armstrong et al., 2014; Barrachina et al., 2006; Cataldo et al., 1991; Piras et al., 2016; Schwagerl et al., 1995) although it is not known if this increase occurs via LE or which cell types this material may have come from. One explanation could be that a sustained reduction in LE and the failure to mount an initial inflammatory response to an increasingly pathogenic environment may contribute to both cell intrinsic or extrinsic compensatory mechanism that ultimately leads to chronic inflammation observed in AD.

4.4 Working model

Altogether, we propose a working model that underpins the abnormal lysosomal phenotypes observed in SORL1 KO hMGLs (Figure 7). Decreased lysosomal degradation caused by impaired trafficking of lysosomal enzymes and decreased lysosomal enzyme activity combined with decreased LE leads to increased lysosomal accumulation of substrates, including fibrillar Aβ 1-42 and synaptosomes, and reduced inflammatory response in microglia with loss of *SORL1*. Depletion of *SORL1* may decrease release of pro-inflammatory cytokines either through conventional secretory routes from the TGN to the cell surface or by impairing LE, as observed in our study. In the context of AD, we posit that lysosome dysfunction in microglia caused by loss of *SORL1* may result in heightened lysosomal stress caused by increased accumulation of substrates and stunted inflammatory response to accumulating pathogenic proteins in the extracellular brain environment. Since loss of *SORL1* is observed in early stages of AD, hypofunctional microglia with depleted SORLA may initially contribute to AD pathogenesis through lysosome dysfunction.

Conclusions

In summary, our study highlights lysosome dysfunction in microglia as a pathway through which *SORL1* loss of function may increase the risk for AD. Our data identifies a previously unexplored cell type-specific mechanism through which *SORL1* can regulate the endo-lysosomal pathway beyond its well-established function as a sorting receptor for APP in neurons, illustrating the importance of exploring this multifaceted sorting receptor and potent AD risk factor as a therapeutic target for AD.

Limitations of the study

We recognize our study has several limitations. *In vitro* studies using hiPSC-derived microglia do not allow thorough representation of cellular complexity characteristics of the physiological brain environment. We acknowledge that since our hMGLs are cultured in isolation, in the absence of neurons and astrocytes, and in two-dimensional cultures, their inflammatory response and morphology may be altered (Baxter et al., 2021). Future work should include studies with hMGLs transplanted into rodent brains or organoid models. Moreover, understanding the interaction of *SORL1* with other AD risk factors in regulating microglia lysosome function will further capture the complexity of AD. Nevertheless, our hiPSC model system has enabled a detailed investigation and provided evidence of cell autonomous role of *SORL1* in regulating microglial lysosome function.

Figure legends

Figure 1. Loss of *SORL1* results in decreased lysosomal degradation in hMGLs. A) Schematic illustrating experimental design using DQ-BSA, a fluorogenic protease substrate that fluoresces only upon lysosomal degradation by proteases. A pulse chase experiment performed with WT and *SORL1* KO hMGLs and Mean fluorescence intensity (MFI) measured using flow cytometry. B) *SORL1* KO hMGLs show decreased MFI of DQ-BSA at all timepoints indicating decreased lysosomal degradation. Lysosomotropic agent chloroquine that inhibits lysosomal degradation was used as control. Chloroquine treatment shows decreased lysosomal degradation of DQ-BSA in both WT and *SORL1* KO hMGLs. C) Flow cytometry showing decreased MFI of BSA-594 in *SORL1* KO hMGLs relative to WT hMGLs suggestive of decreased uptake of BSA in hMGLs with loss of *SORL1*. (D-E) Immunocytochemistry of hMGLs treated with DQ-BSA using the

experimental design in (A), cells fixed for 2h and labeled with the microglia marker, CX3CR1 showing decreased lysosomal degradation in SORL1 KO hMGLs as compared to WT hMGLs, validating results obtained from the experiments using flow cytometry. Similar to the flow cytometry experiment, chloroquine was used as a control and showed decreased MFI in both WT and SORL1 KO hMGLs indicating reduced lysosomal degradation. 2 isogenic clones per genotype (WT and *SORL1* KO) and 9 independent replicates per clone per genotype (N=18 independent replicates) were used for these experiments. Data represented as mean ± SD and analyzed using parametric two-tailed unpaired t test . Significance was defined as a value of *$p < 0.05$, **$p < 0.01$, ***$p < 0.001$, and ****$p < 0.0001$, ns=not significant.

Figure 2. Loss of *SORL1* results in decreased lysosomal enzyme activity in hMGLs. A) Enzyme activity assays based on fluorometric detection show reduced enzyme activity of lysosomal enzymes A) HEXB, B) Cathepsin B and C) Cathepsin D in *SORL1* KO hMGLs as compared to WT hMGLs. Both WT and *SORL1* KO hMGLs show reduced enzyme activity of all the enzymes tested when treated with the lysosome function inhibitor, chloroquine, which was used as a control. (D-F) Western blotting demonstrates no change in total protein levels of immature and mature forms of HEXB, Cathepsin B and Cathepsin D in *SORL1* KO hMGLs relative to WT hMGLs. For the enzyme activity assays, 2 isogenic clones per genotype (WT and *SORL1* KO) and 6 independent replicates per clone per genotype (N=12 independent replicates) were used and for the western blot experiments, 2 isogenic clones per genotype (WT and *SORL1* KO) and 2 independent replicates per clone per genotype (N=4 independent replicates) were utilized. Data represented as mean ± SD and analyzed using parametric two-tailed unpaired t test. Significance was defined as a value of *$p < 0.05$, **$p < 0.01$, ***$p < 0.001$, and ****$p < 0.0001$, ns=not significant.

Figure 3. Loss of *SORL1* results in altered trafficking of lysosomal enzymes in hMGLs Immunocytochemistry and colocalization analysis used to measure colocalization of lysosomal enzymes HEXB, Cathepsin B and Cathepsin D with TGN and lysosomes using TGN38 and LAMP1 antibodies respectively. As compared to WT hMGLs, *SORL1* KO hMGLs show increased colocalization of all the enzymes with TGN38 (Figure 3A,C,E) and decreased colocalization of all enzymes with LAMP1 (Figure 3B,D and F) suggestive of altered trafficking of lysosomal enzymes from TGN to lysosomes. Colocalization was measured using JACOP plugin in Image J software

and presented as Manders correlation coefficient. Scale bar=10μm. 2 isogenic clones per genotype (WT and *SORL1* KO) and 10 images per clone per genotype (N=20 independent replicates) were used for these experiments. Each image comprised of at least 5-10 cells and hence a total of 50-100 cells per clone per genotype were analyzed for colocalization analysis.

Figure 4. Loss of *SORL1* causes reduced lysosomal exocytosis in hMGLs (A-B) Surface expression of LAMP1 measured by immunocytochemistry and flow cytometry as a readout of LE A) Immunocytochemistry with antibody specific for the N terminal luminal epitope of LAMP1 and microglia marker, CX3CR1 demonstrating decreased surface expression of LAMP1 in *SORL1* KO hMGLs as compared to WT hMGLs. B) Quantification by flow cytometry showing decreased MFI of LAMP1 antibody in *SORL1* KO hMGLs relative to WT hMGLs suggestive of decreased LE with loss of *SORL1* in hMGLs. (C-E) Extracellular enzyme activity of lysosomal enzymes measured as a readout of LE. Enzyme activity assays demonstrate decreased lysosomal enzyme activity of C) HEXB, D) Cathepsin B and E) Cathepsin D in *SORL1* KO hMGLs as compared to WT hMGLs suggestive of decreased LE with loss of *SORL1* in hMGLs. 2 isogenic clones per genotype (WT and *SORL1* KO) and 6 independent replicates per clone per genotype (N=12 independent replicates) were used for these experiments. Data represented as mean ± SD and analyzed using parametric two-tailed unpaired t test. Significance was defined as a value of $*p < 0.05$, $**p < 0.01$, $***p < 0.001$, and $****p < 0.0001$, ns=not significant.

Figure 5. Loss of *SORL1* causes increased lysosomal accumulation of fibrillar Aβ 1-42 (fAβ) and synaptosomes in hMGLs. Immunocytochemistry and colocalization analysis showing increased colocalization of (A-B) fAβ and (C-D) synaptosomes with lysosome marker, LAMP1 in *SORL1* KO hMGLs as compared to WT hMGLs suggestive of increased lysosomal accumulation. Colocalization analysis performed using JACOP plugin of Image J software and data is presented as Manders correlation coefficient. Scale bar=10μm. 2 isogenic clones per genotype (WT and *SORL1* KO) and 10 images per clone per genotype (N=20 independent replicates) were used for these experiments. Each image comprised of at least 5-10 cells and hence a total of 50-100 cells per clone per genotype were analyzed for colocalization analysis. (E-H) Immunocytochemistry with hMGLs treated with fibrillar Aβ-647 and CM-Dil dye labeled synaptosomes and co-labeled with microglia marker, CX3CR1 showing increased intracellular phagocytosis of (E) fibrillar Aβ-647 and (G) synaptosomes in *SORL1* KO hMGLs as compared to

WT hMGLs. These findings were further confirmed by flow cytometry. Quantification of Mean fluorescence intensity (MFI) as a readout of phagocytosis in hMGLs treated with both substrates for 30 mins, 5h and 24h demonstrating increased phagocytosis of (F) fibrillar Aβ-647 and (H) synaptosomes in *SORL1* KO hMGLs relative to WT hMGLs. Scale bar = 10μm. 2 isogenic clones per genotype (WT and *SORL1* KO) and 9 independent replicates per clone per genotype (N=18 independent replicates) were used for these experiments. Data represented as mean ± SD and analyzed using parametric two-tailed unpaired *t* test. Significance was defined as a value of $*p < 0.05$, $**p < 0.01$, $***p < 0.001$, and $****p < 0.0001$, ns=not significant.

Figure 6. Loss of *SORL1* results in reduced inflammatory response to pro-inflammatory stimuli in hMGLs. Pro-inflammatory cytokines in the media of hMGLs measured using the Proinflammatory Panel 1 (human) kit (#K15049D; MSD V-PLEX MULTI-SPOT assay System) showing decreased levels of cytokines released into the media in SORL1 KO hMGLs as compared to WT hMGLs in response to pro-inflammatory stimuli, LPS and IFN-γ. These cytokines include (A) IL-1β and (B) IL-12p70 known to be secreted via lysosomal exocytosis and (C-G) the pro-inflammatory cytokines IL-6, IL-15, IP-10, TNF-α and IL-8 and (H-J) anti-inflammatory cytokines IL-10, IL-13, and IL-2 known to be secreted by LE independent pathways including regulated and constitute exocytosis. Unstimulated *SORL1* KO hMGLs demonstrated reduced extracellular levels of (A-D) IL-6, IL-2p70 (IL-12), IP-10 and IL-1β but no change in (E-J) IL-10, IL-8, IL-15, IL-13, IL-2 and TNF-α (E-J) as compared to WT hMGLs. 2 isogenic clones per genotype (WT and *SORL1* KO) and 6 independent replicates per clone per genotype (N=12 independent replicates) were used for these experiments. Data represented as mean ± SD and analyzed using parametric two-tailed unpaired *t* test. Significance was defined as a value of $*p < 0.05$, $**p < 0.01$, $***p < 0.001$, and $****p < 0.0001$, ns=not significant.

Figure 7. Working model. We propose the following working model that underpins the abnormal lysosomal phenotype observed in *SORL1* KO hMGLs. Decreased lysosomal degradation caused by impaired trafficking of lysosomal enzymes and decreased lysosomal enzyme activity, combined with decreased lysosomal exocytosis, leads to increased lysosomal accumulation of substrates including fibrillar Aβ 1-42 and synaptosomes and reduced pro-inflammatory response in microglia with loss of *SORL1*. Depletion of *SORL1* may decrease release of pro-inflammatory cytokines

either through conventional secretory routes from TGN to the cell surface or by impairing LE, as observed in our study. Altogether, loss of *SORL1* causes increased lysosomal stress in human microglia.

Supplementary information

Supplementary methods

Differentiation of microglia from hiPSCs using Dolan et al 2023 protocol.

hMGLs were also generated using a different iPSC-microglia differentiation protocol (Dolan et al., 2023). Briefly, hiPSCs were cultured in E8 media (Gibco #A1517001), dissociated with accutase and seeded in E8 media with rock inhibitor (RI; SelleckChem #S1049) at a density of 300k cells / well in ultra-low attachment plates (VWR #29443-030) to form embryoid bodies (EBs; DIV-1). EBs were cultured DIV0 to DIV4 in hypoxia (5% O_2, 5% CO_2, 37°C) and DIV4-DIV in normoxia (20% O_2, 5% CO_2, 37°C). EBs were given a full media change on DIV0 and cultured to DIV10 in iHPC media (1:1 IMDM:F12, 2% ITSG-X, 1% Glutamax, 1% Chemically-defined lipid concentrate, 1% NEAA, 10 ug/mL Poly(vinyl alchohol), 400 uM Monothioglycerol, 64 ug/mL L-ascorbic acid 2-Phosphate). On DIV0, EBs were treated with 50 ng/mL FGF2 (Gibco #PHG0261), 50 ng/mL BMP4 (Gibco #PHC9534), 12.5 ng/mL Activin-A (Gibco #PHC9564), 1 uM RI, 2 uM LiCl (Sigma #L7026). On DIV2, EBs were treated with 50 ng/mL VEGF (Peprotech #100-20), 50 ng/mL FGF2. On DIV4, DIV6, DIV8, EBs were treated with 50 ng/mL FGF2, 50 ng/mL VEGF, 10 ng/mL SCF (Gibco #PHC2116), 50 ng/mL TPO (Peprotech #300-18), 10 ng/mL IL-3 (Peprotech #200-03), 50 ng/mL IL-6 (Peprotech #AF-200-06). EBs were given a full media change on DIV0, DIV2, and DIV4 (2 mL / 6w), and media was added on top on DIV6 and DIV8 (1 mL / 6w). Floating iHPCs were separated from gravity-settled EBs by filtering through 40 um filter. iHPCs were counted with a Countess 3 (Invitrogen #AMQAX2000) and frozen in CryoStor CS10

(Stem Cell Technologies #07930). To differentiate into hMGLs, HPCs were thawed onto growth factor reduced matrigel-coated plates in 2 mL / 6w at a density of 100k / 6w in iMBM media (DMEM/F12, 2% ITS-G, 2% B-27, 1% N-2, 200 uM Monothioglycerol, 1% Glutamax, 1% NEAA, 5 ug / mL Insulin) with 50 ng/mL TGFB1 (Peprotech #100-21), 100 ng/mL IL-34 (BioLegend #577906), 25 ng/mL M-CSF (Peprotech #AF-300-25). hMGLs were given media additions with fresh cytokines (1 mL / 6w) every 2 days. hMGLs were re-plated on DIV22 and DIV30 at a density of 130k / 6w in 1:1 conditioned media and fresh media. hMGLs were re-plated by collecting floating cells, incubating attached cells in PBS for 5 minutes, and lifting attached wells with a cell lifter (VWR #29442-200). iMGL media was supplemented with 100 ng/mL CD200 (Bon Opus #C311) and 100 ng/mL CX3CL1 (Peprotech #300-31) beginning on DIV30 to promote microglial maturation.

Characterization of hiPSC-derived microglia generated using Dolan et al 2023 protocol.

Differentiation of hMGLs from hiPSCs and HPCs was assessed at DIV22 (iMGL expression of CD33, P2RY12, CX3CR1, and high CD45) by flow cytometry. Surface markers were assessed by lifting cells and suspending in 5% BSA in PBS with 1:100 Fc Block (BioLegend Cat#422302). Cells were stained with pre-conjugated primary antibodies at 1:100 dilution for 15 min at 4°C. Primaries antibodies used were: P2RY12-PE (BioLegend Cat# 392103), CX3CR1-PE (BioLegend Cat# 341603), CD33-PE/Cy7 (BioLegend Cat# 303402), and CD45-488 (BioLegend Cat# 304019). Cells were washed once with PBS and resuspended in 0.1% BSA in PBS with 1 µg/mL DAPI (Cayman Chemicals Cat# 14285-5). Flow cytometry data was collected on a Cytoflex LX analyzer (Beckman Coulter). Cells were identified by gating on FSC-A vs. SSC-A, singlets by FSC-A vs. FSC-H, and live cells by V450-A vs. SSC-A. Marker percentage positive was quantified by gating PE/Cy7 fluorescence channels using DAPI-only staining controls for each sample replicate.

Lysosomal enzyme activity assay using hiPSC-derived microglia generated using Dolan et al 2023 protocol. For enzyme activity assays performed with hMGLs generated using the protocol based on Dolan et al 2023, conditioned media was collected from hMGLs at DIV40, centrifuged at 300g for 5 minutes, and frozen at -80°C. hMGLs were lifted as described above and centrifuged at 300g for 5 minutes, supernatant removed, and cell pellets lysed in CD Lysis buffer (300 uL / 12-well). Lysates were centrifuged at 20,000g for 15 min at 4°C to pellet debris and then frozen at -

80°C. Conditioned media and lysates were thawed on ice and aliquoted into a 96-well (Corning #3904; 50 uL/well, 2 replicate wells/sample). CTSD substrate (Abcam #ab65300) or HEXB substrate (Cell Biolabs #MET-5095) was added to wells (50 uL/well) and plates were incubated at 37°C for 30 minutes. Neutralization reagent (100 uL/well) was added to HEXB assay wells. Sample fluorescence was measured using a Perkin Elmer EnSpire Plate Reader. CTSD: Ex 328 / Em 460; HEXB: Ex 365 / Em 460. Fluorescence values were averaged between replicate wells.

<u>Supplementary Figure legends</u>

Supplementary figure 1. Characterization of Hematopoietic progenitor cells (HPCs) and microglia derived from hiPSCs (hMGLs) with loss of *SORL1* A) Schematic showing protocol used for derivation of HPCs and microglia from hiPSCs. Protocol was based on (McQuade et al., 2018) with some modifications B) Histogram generated using FlowJo showing positive expression of HPC marker, CD43 in both WT and *SORL1* KO hMGLs. C) Brightfield images at 10X and 20X magnifications, showing HPCs (bright grape like clusters) derived from WT and *SORL1* KO hiPSCs. D) Mean fluorescence intensity measured by flow cytometry showing no difference in expression of HPC marker, CD43 in WT and *SORL1* KO hMGLs. E) Immunocytochemistry showing positive expression of microglia specific markers including Iba1, P2RY12 TMEM119 and CX3CR1 in both WT and *SORL1* KO hMGLs. Images were acquired using confocal microscopy and Leica software. Scale bar = 10µm. 2 isogenic clones per genotype (WT and *SORL1* KO) and 9 independent replicates per clone per genotype (N=18 independent replicates) were used for these experiments. Data represented as mean ± SD and analyzed using parametric two-tailed unpaired *t* test. Significance was defined as a value of $*p < 0.05$, $**p < 0.01$, $***p < 0.001$, and $****p < 0.0001$, ns=not significant.

Supplementary figure 2. Loss of *SORL1* results in reduced intracellular enzyme activity of CTSD and decreased extracellular enzyme activity of CTSD and HEXB lysosomal enzymes in hMGLs generated using Dolan et al protocol A) Expression of microglia specific markers, CD33, P2RY12, CX3CR1 and CD45 high assessed by flow cytometry. Enzyme activity assays showing B) Reduced intracellular enzyme activity of CTSD; (C-D) Reduced extracellular enzyme activity of CTSD and HEXB indicating reduced LE in *SORL1* KO hMGLs as compared to WT hMGLs. 1 clone per genotype (WT and *SORL1* KO) and 6 independent replicates per clone per genotype (N=6 independent replicates) were used for these experiments. Data represented as

mean ± SD and analyzed using parametric two-tailed unpaired *t* test. Significance was defined as a value of *$p < 0.05$, **$p < 0.01$, ***$p < 0.001$, and ****$p < 0.0001$, ns=not significant.

Supplementary figure 3. Loss of *SORL1* results in decreased intensity of Aβ-phrodo in *SORL1* KO hMGLs A) Schematic of experimental design showing pulse chase assay used for treating cells with fAβ-Phrodo B) Flow cytometry used to measure fluorescence intensity of Phrodo conjugated to fAβ reveals no difference in Phrodo intensity at time 0 but decreased fluorescence intensity of pHrodo after a chase period of 30 min, 2h and 5h in *SORL1* KO hMGLs. 2 isogenic clones per genotype (WT and *SORL1* KO) and 9 independent replicates per clone per genotype (N=18 independent replicates) were used for these experiments. Data represented as mean ± SD and analyzed using parametric two-tailed unpaired *t* test. Significance was defined as a value of *$p < 0.05$, **$p < 0.01$, ***$p < 0.001$, and ****$p < 0.0001$, ns=not significant.

References

2023 Alzheimer's disease facts and figures. (2023). *Alzheimers Dement*, *19*(4), 1598-1695. https://doi.org/10.1002/alz.13016

Akiyama, H., Mori, H., Saido, T., Kondo, H., Ikeda, K., & McGeer, P. L. (1999). Occurrence of the diffuse amyloid β-protein (Aβ) deposits with numerous Aβ-containing glial cells in the cerebral cortex of patients with Alzheimer's disease. *Glia*, *25*(4), 324-331.

Allendorf, D. H., & Brown, G. C. (2022). Neu1 Is Released From Activated Microglia, Stimulating Microglial Phagocytosis and Sensitizing Neurons to Glutamate [Original Research]. *Frontiers in cellular neuroscience*, *16*. https://doi.org/10.3389/fncel.2022.917884

Amos, P. J., Fung, S., Case, A., Kifelew, J., Osnis, L., Smith, C. L., Green, K., Naydenov, A., Aloi, M., Hubbard, J. J., Ramakrishnan, A., Garden, G. A., & Jayadev, S. (2017). Modulation of Hematopoietic Lineage Specification Impacts TREM2 Expression in Microglia-Like Cells Derived From Human Stem Cells. *ASN Neuro*, *9*(4), 1759091417716610. https://doi.org/10.1177/1759091417716610

Andersen, O. M., Bøgh, N., Landau, A. M., Pløen, G. G., Jensen, A. M. G., Monti, G., Ulhøi, B. P., Nyengaard, J. R., Jacobsen, K. R., Jørgensen, M. M., Holm, I. E., Kristensen, M. L., Alstrup, A. K. O., Hansen, E. S. S., Teunissen, C. E., Breidenbach, L., Droescher, M., Liu, Y., Pedersen, H. S., . . . Sørensen, C. B. (2022). A genetically modified minipig model for Alzheimer's disease with SORL1 haploinsufficiency. *Cell Reports Medicine*, *3*(9), 100740. https://doi.org/https://doi.org/10.1016/j.xcrm.2022.100740

Andrei, C., Margiocco, P., Poggi, A., Lotti, L. V., Torrisi, M. R., & Rubartelli, A. (2004). Phospholipases C and A2 control lysosome-mediated IL-1β secretion: implications for inflammatory processes. *Proceedings of the National Academy of Sciences*, *101*(26), 9745-9750.

Andrews, N. W. (2017). Detection of Lysosomal Exocytosis by Surface Exposure of Lamp1 Luminal Epitopes. *Methods in molecular biology (Clifton, N.J.)*, *1594*, 205-211. https://doi.org/10.1007/978-1-4939-6934-0_13

Arighi, C. N., Hartnell, L. M., Aguilar, R. C., Haft, C. R., & Bonifacino, J. S. (2004). Role of the mammalian retromer in sorting of the cation-independent mannose 6-phosphate receptor. *The Journal of cell biology*, *165*(1), 123-133. https://doi.org/10.1083/jcb.200312055

Armstrong, A., Mattsson, N., Appelqvist, H., Janefjord, C., Sandin, L., Agholme, L., Olsson, B., Svensson, S., Blennow, K., Zetterberg, H., & Kågedal, K. (2014). Lysosomal network proteins as potential novel CSF biomarkers for Alzheimer's disease. *Neuromolecular Med*, *16*(1), 150-160. https://doi.org/10.1007/s12017-013-8269-3

Barrachina, M., Maes, T., Buesa, C., & Ferrer, I. (2006). Lysosome-associated membrane protein 1 (LAMP-1) in Alzheimer's disease. *Neuropathol Appl Neurobiol*, *32*(5), 505-516. https://doi.org/10.1111/j.1365-2990.2006.00756.x

Baxter, P. S., Dando, O., Emelianova, K., He, X., McKay, S., Hardingham, G. E., & Qiu, J. (2021). Microglial identity and inflammatory responses are controlled by the combined effects of neurons and astrocytes. *Cell Rep*, *34*(12), 108882. https://doi.org/10.1016/j.celrep.2021.108882

Beeken, J., Kessels, S., Rigo, J. M., Alpizar, Y. A., Nguyen, L., & Brône, B. (2022). p27(kip1) Modulates the Morphology and Phagocytic Activity of Microglia. *International journal of molecular sciences*, *23*(18). https://doi.org/10.3390/ijms231810432

Binkle, L., Klein, M., Borgmeyer, U., Kuhl, D., & Hermey, G. (2022). The adaptor protein PICK1 targets the sorting receptor SorLA. *Molecular Brain*, *15*(1), 18. https://doi.org/10.1186/s13041-022-00903-0

Blott, E. J., & Griffiths, G. M. (2002). Secretory lysosomes. *Nature reviews Molecular cell biology*, *3*(2), 122-131.

Bolmont, T., Haiss, F., Eicke, D., Radde, R., Mathis, C. A., Klunk, W. E., Kohsaka, S., Jucker, M., & Calhoun, M. E. (2008). Dynamics of the microglial/amyloid interaction indicate a role in plaque maintenance. *Journal of Neuroscience*, *28*(16), 4283-4292.

Braulke, T., & Bonifacino, J. S. (2009). Sorting of lysosomal proteins. *Biochimica et Biophysica Acta (BBA) - Molecular Cell Research*, *1793*(4), 605-614. https://doi.org/https://doi.org/10.1016/j.bbamcr.2008.10.016

Burgert, T., Schmidt, V., Caglayan, S., Lin, F., Füchtbauer, A., Füchtbauer, E. M., Nykjaer, A., Carlo, A. S., & Willnow, T. E. (2013). SORLA-dependent and -independent functions for PACS1 in control of amyloidogenic processes. *Mol Cell Biol*, *33*(21), 4308-4320. https://doi.org/10.1128/mcb.00628-13

Campion, D., Charbonnier, C., & Nicolas, G. (2019). SORL1 genetic variants and Alzheimer disease risk: a literature review and meta-analysis of sequencing data. *Acta Neuropathologica*, *138*(2), 173-186.

Cataldo, A. M., Paskevich, P. A., Kominami, E., & Nixon, R. A. (1991). Lysosomal hydrolases of different classes are abnormally distributed in brains of patients with Alzheimer disease. *Proceedings of the National Academy of Sciences*, *88*(24), 10998-11002. https://doi.org/10.1073/pnas.88.24.10998

Cermak, S., Kosicek, M., Mladenovic-Djordjevic, A., Smiljanic, K., Kanazir, S., & Hecimovic, S. (2016). Loss of Cathepsin B and L Leads to Lysosomal Dysfunction, NPC-Like Cholesterol Sequestration and Accumulation of the Key Alzheimer's Proteins. *PLOS ONE*, *11*(11), e0167428. https://doi.org/10.1371/journal.pone.0167428

Chen, H. J., Yuan, J., & Lobel, P. (1997). Systematic mutational analysis of the cation-independent mannose 6-phosphate/insulin-like growth factor II receptor cytoplasmic domain: an acidic cluster containing a key aspartate is important for function in lysosomal enzyme sorting. *Journal of Biological Chemistry*, *272*(11), 7003-7012.

Chiaruttini, G., Piperno, G. M., Jouve, M., De Nardi, F., Larghi, P., Peden, A. A., Baj, G., Müller, S., Valitutti, S., Galli, T., & Benvenuti, F. (2016). The SNARE VAMP7 Regulates Exocytic Trafficking of Interleukin-12 in Dendritic Cells. *Cell Rep*, *14*(11), 2624-2636. https://doi.org/10.1016/j.celrep.2016.02.055

Cooper, A. A., & Stevens, T. H. (1996). Vps10p cycles between the late-Golgi and prevacuolar compartments in its function as the sorting receptor for multiple yeast vacuolar hydrolases. *The Journal of cell biology*, *133*(3), 529-541.

Cui, Y., Carosi, J. M., Yang, Z., Ariotti, N., Kerr, M. C., Parton, R. G., Sargeant, T. J., & Teasdale, R. D. (2019). Retromer has a selective function in cargo sorting via endosome transport carriers. *The Journal of cell biology*, *218*(2), 615-631. https://doi.org/10.1083/jcb.201806153

Di Spiezio, A., Marques, A. R., Schmidt, L., Thießen, N., Gallwitz, L., Fogh, J., Bartsch, U., & Saftig, P. (2021). Analysis of cathepsin B and cathepsin L treatment to clear toxic lysosomal protein aggregates in neuronal ceroid lipofuscinosis. *Biochimica et Biophysica Acta (BBA)-Molecular Basis of Disease*, *1867*(10), 166205.

Dodson, S. E., Gearing, M., Lippa, C. F., Montine, T. J., Levey, A. I., & Lah, J. J. (2006). LR11/SorLA expression is reduced in sporadic Alzheimer disease but not in familial Alzheimer disease. *Journal of neuropathology and experimental neurology*, *65*(9), 866-872. https://doi.org/10.1097/01.jnen.0000228205.19915.20

Dolan, M.-J., Therrien, M., Jereb, S., Kamath, T., Gazestani, V., Atkeson, T., Marsh, S. E., Goeva, A., Lojek, N. M., Murphy, S., White, C. M., Joung, J., Liu, B., Limone, F., Eggan, K., Hacohen, N., Bernstein, B. E., Glass, C. K., Leinonen, V., . . . Stevens, B. (2023). Exposure of iPSC-derived human microglia to brain substrates enables the generation and manipulation of diverse transcriptional states in vitro. *Nature Immunology*, *24*(8), 1382-1390. https://doi.org/10.1038/s41590-023-01558-2

Fjorback, A. W., Seaman, M., Gustafsen, C., Mehmedbasic, A., Gokool, S., Wu, C., Militz, D., Schmidt, V., Madsen, P., & Nyengaard, J. R. (2012). Retromer binds the FANSHY sorting motif in SorLA to regulate amyloid precursor protein sorting and processing. *Journal of Neuroscience*, *32*(4), 1467-1480.

Gardella, S., Andrei, C., Lotti, L. V., Poggi, A., Torrisi, M. R., Zocchi, M. R., & Rubartelli, A. (2001). CD8+ T lymphocytes induce polarized exocytosis of secretory lysosomes by dendritic cells with release of interleukin-1β and cathepsin D. *Blood*, *98*(7), 2152-2159. https://doi.org/10.1182/blood.V98.7.2152

Hamazaki, H. (1996). Cathepsin D is involved in the clearance of Alzheimer's beta-amyloid protein. *FEBS letters*, *396*(2-3), 139-142. https://doi.org/10.1016/0014-5793(96)01087-3

Holstege, H., van der Lee, S. J., Hulsman, M., Wong, T. H., van Rooij, J. G. J., Weiss, M., Louwersheimer, E., Wolters, F. J., Amin, N., Uitterlinden, A. G., Hofman, A., Ikram, M. A., van Swieten, J. C., Meijers-Heijboer, H., van der Flier, W. M., Reinders, M. J. T., van Duijn, C. M., & Scheltens, P. (2017). Characterization of pathogenic SORL1 genetic variants for association with Alzheimer's disease: a clinical interpretation strategy. *European Journal of Human Genetics*, *25*(8), 973-981. https://doi.org/10.1038/ejhg.2017.87

Holstege, H., Waal, M. W. J. d., Tesi, N., Lee, S. J. v. d., ADES-consortium, consortium, A., consortium, S.-A., Knight-ADRC, UCSF/NYGC/UAB, Vogel, M., Spaendonk, R. v., Hulsman, M., & Andersen, O. M. (2023). Effect of prioritized SORL1

missense variants supports clinical consideration for familial Alzheimer's Disease. *medRxiv*, 2023.2007.2013.23292622. https://doi.org/10.1101/2023.07.13.23292622

Hung, C., Tuck, E., Stubbs, V., van der Lee, S. J., Aalfs, C., van Spaendonk, R., Scheltens, P., Hardy, J., Holstege, H., & Livesey, F. J. (2021). SORL1 deficiency in human excitatory neurons causes APP-dependent defects in the endolysosome-autophagy network. *Cell reports*, *35*(11).

Ii, K., Ito, H., Kominami, E., & Hirano, A. (1993). Abnormal distribution of cathepsin proteinases and endogenous inhibitors (cystatins) in the hippocampus of patients with Alzheimer's disease, parkinsonism-dementia complex on Guam, and senile dementia and in the aged. *Virchows Arch A Pathol Anat Histopathol*, *423*(3), 185-194. https://doi.org/10.1007/bf01614769

Itagaki, S., McGeer, P., Akiyama, H., Zhu, S., & Selkoe, D. (1989). Relationship of microglia and astrocytes to amyloid deposits of Alzheimer disease. *Journal of neuroimmunology*, *24*(3), 173-182.

Iyer, H., Shen, K., Meireles, A. M., & Talbot, W. S. (2022). A lysosomal regulatory circuit essential for the development and function of microglia. *Science Advances*, *8*(35), eabp8321.

Jacobsen, L., Madsen, P., Jacobsen, C., Nielsen, M. S., Gliemann, J., & Petersen, C. M. (2001). Activation and functional characterization of the mosaic receptor SorLA/LR11. *Journal of Biological Chemistry*, *276*(25), 22788-22796.

Jacobsen, L., Madsen, P., Moestrup, S. K., Lund, A. H., Tommerup, N., Nykjær, A., Sottrup-Jensen, L., Gliemann, J., & Petersen, C. M. (1996). Molecular characterization of a novel human hybrid-type receptor that binds the α2-macroglobulin receptor-associated protein. *Journal of Biological Chemistry*, *271*(49), 31379-31383.

Keilani, S., Lun, Y., Stevens, A. C., Williams, H. N., Sjoberg, E. R., Khanna, R., Valenzano, K. J., Checler, F., Buxbaum, J. D., Yanagisawa, K., Lockhart, D. J., Wustman, B. A., & Gandy, S. (2012). Lysosomal Dysfunction in a Mouse Model of Sandhoff Disease Leads to Accumulation of Ganglioside-Bound Amyloid-β Peptide. *The Journal of Neuroscience*, *32*(15), 5223-5236. https://doi.org/10.1523/jneurosci.4860-11.2012

Kenessey, A., Nacharaju, P., Ko, L. w., & Yen, S. H. (1997). Degradation of tau by lysosomal enzyme cathepsin D: implication for Alzheimer neurofibrillary degeneration. *Journal of Neurochemistry*, *69*(5), 2026-2038.

Knupp, A., Mishra, S., Martinez, R., Braggin, J. E., Szabo, M., Kinoshita, C., Hailey, D. W., Small, S. A., Jayadev, S., & Young, J. E. (2020). Depletion of the AD Risk Gene SORL1 Selectively Impairs Neuronal Endosomal Traffic Independent of Amyloidogenic APP Processing. *Cell reports*, *31*(9), 107719. https://doi.org/https://doi.org/10.1016/j.celrep.2020.107719

Koike, M., Nakanishi, H., Saftig, P., Ezaki, J., Isahara, K., Ohsawa, Y., Schulz-Schaeffer, W., Watanabe, T., Waguri, S., Kametaka, S., Shibata, M., Yamamoto, K., Kominami, E., Peters, C., von Figura, K., & Uchiyama, Y. (2000). Cathepsin D deficiency induces lysosomal storage with ceroid lipofuscin in mouse CNS neurons. *The Journal of neuroscience : the official journal of the Society for Neuroscience*, *20*(18), 6898-6906. https://doi.org/10.1523/jneurosci.20-18-06898.2000

Kuil, L. E., López Martí, A., Carreras Mascaro, A., van den Bosch, J. C., van den Berg, P., van der Linde, H. C., Schoonderwoerd, K., Ruijter, G. J. G., & van Ham, T. J. (2019). Hexb enzyme deficiency leads to lysosomal abnormalities in radial glia and microglia in zebrafish brain development. *Glia*, *67*(9), 1705-1718. https://doi.org/10.1002/glia.23641

Kunkle, B. W., Vardarajan, B. N., Naj, A. C., Whitehead, P. L., Rolati, S., Slifer, S., Carney, R. M., Cuccaro, M. L., Vance, J. M., Gilbert, J. R., Wang, L.-S., Farrer, L. A., Reitz, C., Haines, J. L., Beecham, G. W., Martin, E. R., Schellenberg, G. D., Mayeux, R. P., & Pericak-Vance, M. A. (2017). Early-Onset Alzheimer Disease and Candidate Risk Genes Involved in Endolysosomal Transport. *JAMA neurology*, *74*(9), 1113-1122. https://doi.org/10.1001/jamaneurol.2017.1518

Lambert, J.-C., Ibrahim-Verbaas, C. A., Harold, D., Naj, A. C., Sims, R., Bellenguez, C., Jun, G., DeStefano, A. L., Bis, J. C., Beecham, G. W., Grenier-Boley, B., Russo, G., Thornton-Wells, T. A., Jones, N., Smith, A. V., Chouraki, V., Thomas, C., Ikram, M. A., Zelenika, D., . . . Aging Research in Genomic, E. (2013). Meta-analysis of 74,046 individuals identifies 11 new susceptibility loci for Alzheimer's disease. *Nature genetics*, *45*(12), 1452-1458. https://doi.org/10.1038/ng.2802

Lancaster, C. E., Fountain, A., Dayam, R. M., Somerville, E., Sheth, J., Jacobelli, V., Somerville, A., Terebiznik, M. R., & Botelho, R. J. (2021). Phagosome resolution regenerates lysosomes and maintains the degradative capacity in phagocytes. *Journal of Cell Biology*, *220*(9). https://doi.org/10.1083/jcb.202005072

Lee, H., Aylward, A. J., Pearse, R. V., 2nd, Lish, A. M., Hsieh, Y. C., Augur, Z. M., Benoit, C. R., Chou, V., Knupp, A., Pan, C., Goberdhan, S., Duong, D. M., Seyfried, N. T., Bennett, D. A., Taga, M. F., Huynh, K., Arnold, M., Meikle, P. J., De Jager, P. L., . . . Young-Pearse, T. L. (2023). Cell-type-specific regulation of APOE and CLU levels in human neurons by the Alzheimer's disease risk gene SORL1. *Cell Rep*, *42*(8), 112994. https://doi.org/10.1016/j.celrep.2023.112994

Liu, T., Zhu, B., Liu, Y., Zhang, X., Yin, J., Li, X., Jiang, L., Hodges, A. P., Rosenthal, S. B., Zhou, L., Yancey, J., McQuade, A., Blurton-Jones, M., Tanzi, R. E., Huang, T. Y., & Xu, H. (2020). Multi-omic comparison of Alzheimer's variants in human ESC-derived microglia reveals convergence at APOE. *J Exp Med*, *217*(12). https://doi.org/10.1084/jem.20200474

Maninger, J.-K., Nowak, K., Goberdhan, S., O'Donoghue, R., & Connor-Robson, N. (2024). Cell type-specific functions of Alzheimer's disease endocytic risk genes. *Philosophical Transactions of the Royal Society B*, *379*(1899), 20220378.

Marwaha, R., & Sharma, M. (2017). DQ-Red BSA Trafficking Assay in Cultured Cells to Assess Cargo Delivery to Lysosomes. *Bio-protocol*, *7*(19), e2571. https://doi.org/10.21769/BioProtoc.2571

McQuade, A., & Blurton-Jones, M. (2019). Microglia in Alzheimer's Disease: Exploring How Genetics and Phenotype Influence Risk. *Journal of Molecular Biology*, *431*(9), 1805-1817. https://doi.org/https://doi.org/10.1016/j.jmb.2019.01.045

McQuade, A., Coburn, M., Tu, C. H., Hasselmann, J., Davtyan, H., & Blurton-Jones, M. (2018). Development and validation of a simplified method to generate human microglia from pluripotent stem cells. *Molecular Neurodegeneration*, *13*(1), 67. https://doi.org/10.1186/s13024-018-0297-x

Meyer-Luehmann, M., Spires-Jones, T. L., Prada, C., Garcia-Alloza, M., De Calignon, A., Rozkalne, A., Koenigsknecht-Talboo, J., Holtzman, D. M., Bacskai, B. J., & Hyman, B.

T. (2008). Rapid appearance and local toxicity of amyloid-β plaques in a mouse model of Alzheimer's disease. *Nature*, *451*(7179), 720-724.

Mishra, S. (2024). Differential effects of SORL1 deficiency on the endo-lysosomal network in human neurons and microglia. *Phil. Trans. R. Soc.* https://doi.org/37920220389

Mishra, S., Jayadev, S., & Young, J. E. (2024). Differential effects of SORL1 deficiency on the endo-lysosomal network in human neurons and microglia. *Philos Trans R Soc Lond B Biol Sci*, *379*(1899), 20220389. https://doi.org/10.1098/rstb.2022.0389

Mishra, S., Knupp, A., Kinoshita, C., Williams, C. A., Rose, S. E., Martinez, R., Theofilas, P., & Young, J. E. (2023). Pharmacologic Stabilization of Retromer Rescues Endosomal Pathology Induced by Defects in the Alzheimer's gene SORL1. *bioRxiv*, 2022.2007.2031.502217. https://doi.org/10.1101/2022.07.31.502217

Mishra, S., Knupp, A., Szabo, M. P., Williams, C. A., Kinoshita, C., Hailey, D. W., Wang, Y., Andersen, O. M., & Young, J. E. (2022). The Alzheimer's gene SORL1 is a regulator of endosomal traffic and recycling in human neurons. *Cell Mol Life Sci*, *79*(3), 162. https://doi.org/10.1007/s00018-022-04182-9

Monif, M., Reid, C. A., Powell, K. L., Drummond, K. J., O'Brien, T. J., & Williams, D. A. (2016). Interleukin-1β has trophic effects in microglia and its release is mediated by P2X7R pore. *Journal of neuroinflammation*, *13*(1), 173. https://doi.org/10.1186/s12974-016-0621-8

Nicolas, G., Charbonnier, C., Wallon, D., Quenez, O., Bellenguez, C., Grenier-Boley, B., Rousseau, S., Richard, A.-C., Rovelet-Lecrux, A., & Le Guennec, K. (2016). SORL1 rare variants: a major risk factor for familial early-onset Alzheimer's disease. *Molecular psychiatry*, *21*(6), 831-836.

Nielsen, M. S., Gustafsen, C., Madsen, P., Nyengaard, J. R., Hermey, G., Bakke, O., Mari, M., Schu, P., Pohlmann, R., Dennes, A., & Petersen, C. M. (2007). Sorting by the cytoplasmic domain of the amyloid precursor protein binding receptor SorLA. *Mol Cell Biol*, *27*(19), 6842-6851. https://doi.org/10.1128/mcb.00815-07

Oberstein, T. J., Utz, J., Spitzer, P., Klafki, H. W., Wiltfang, J., Lewczuk, P., Kornhuber, J., & Maler, J. M. (2021). The Role of Cathepsin B in the Degradation of Aβ and in the Production of Aβ Peptides Starting With Ala2 in Cultured Astrocytes [Original Research]. *Frontiers in Molecular Neuroscience*, *13*. https://doi.org/10.3389/fnmol.2020.615740

Olah, M., Patrick, E., Villani, A.-C., Xu, J., White, C. C., Ryan, K. J., Piehowski, P., Kapasi, A., Nejad, P., & Cimpean, M. (2018). A transcriptomic atlas of aged human microglia. *Nature communications*, *9*(1), 539.

Park, J.-C., Han, S.-H., & Mook-Jung, I. (2020). Peripheral inflammatory biomarkers in Alzheimer’s disease: a brief review. *BMB Reports*, *53*(1), 10-19. https://doi.org/10.5483/BMBRep.2020.53.1.309

Perry, V. H., & Holmes, C. (2014). Microglial priming in neurodegenerative disease. *Nature Reviews Neurology*, *10*(4), 217-224.

Piras, A., Collin, L., Grüninger, F., Graff, C., & Rönnbäck, A. (2016). Autophagic and lysosomal defects in human tauopathies: analysis of post-mortem brain from patients with familial Alzheimer disease, corticobasal degeneration and progressive supranuclear palsy. *Acta neuropathologica communications*, *4*, 22. https://doi.org/10.1186/s40478-016-0292-9

Pottier, C., Hannequin, D., Coutant, S., Rovelet-Lecrux, A., Wallon, D., Rousseau, S., Legallic, S., Paquet, C., Bombois, S., & Pariente, J. (2012). High frequency of potentially pathogenic SORL1 mutations in autosomal dominant early-onset Alzheimer disease. *Molecular psychiatry*, *17*(9), 875-879.

Quick, J. D., Silva, C., Wong, J. H., Lim, K. L., Reynolds, R., Barron, A. M., Zeng, J., & Lo, C. H. (2023). Lysosomal acidification dysfunction in microglia: an emerging pathogenic mechanism of neuroinflammation and neurodegeneration. *Journal of neuroinflammation*, *20*(1), 185. https://doi.org/10.1186/s12974-023-02866-y

Reis, R. C., Sorgine, M. H., & Coelho-Sampaio, T. (1998). A novel methodology for the investigation of intracellular proteolytic processing in intact cells. *Eur J Cell Biol*, *75*(2), 192-197. https://doi.org/10.1016/s0171-9335(98)80061-7

Rogaeva, E., Meng, Y., Lee, J. H., Gu, Y., Kawarai, T., Zou, F., Katayama, T., Baldwin, C. T., Cheng, R., Hasegawa, H., Chen, F., Shibata, N., Lunetta, K. L., Pardossi-Piquard, R., Bohm, C., Wakutani, Y., Cupples, L. A., Cuenco, K. T., Green, R. C., . . . St George-Hyslop, P. (2007). The neuronal sortilin-related receptor SORL1 is genetically associated with Alzheimer disease. *Nature genetics*, *39*(2), 168-177. https://doi.org/10.1038/ng1943

Scheltens, P., De Strooper, B., Kivipelto, M., Holstege, H., Chételat, G., Teunissen, C. E., Cummings, J., & van der Flier, W. M. (2021). Alzheimer's disease. *Lancet*, *397*(10284), 1577-1590. https://doi.org/10.1016/s0140-6736(20)32205-4

Scherzer, C. R., Offe, K., Gearing, M., Rees, H. D., Fang, G., Heilman, C. J., Schaller, C., Bujo, H., Levey, A. I., & Lah, J. J. (2004). Loss of Apolipoprotein E Receptor LR11 in Alzheimer Disease. *Archives of Neurology*, *61*(8), 1200-1205. https://doi.org/10.1001/archneur.61.8.1200

Schindelin, J., Arganda-Carreras, I., Frise, E., Kaynig, V., Longair, M., Pietzsch, T., Preibisch, S., Rueden, C., Saalfeld, S., Schmid, B., Tinevez, J. Y., White, D. J., Hartenstein, V., Eliceiri, K., Tomancak, P., & Cardona, A. (2012). Fiji: an open-source platform for biological-image analysis. *Nat Methods*, *9*(7), 676-682. https://doi.org/10.1038/nmeth.2019

Schwagerl, A. L., Mohan, P. S., Cataldo, A. M., Vonsattel, J. P., Kowall, N. W., & Nixon, R. A. (1995). Elevated levels of the endosomal-lysosomal proteinase cathepsin D in cerebrospinal fluid in Alzheimer disease. *J Neurochem*, *64*(1), 443-446. https://doi.org/10.1046/j.1471-4159.1995.64010443.x

Scott, G. K., Fei, H., Thomas, L., Medigeshi, G. R., & Thomas, G. (2006). A PACS-1, GGA3 and CK2 complex regulates CI-MPR trafficking. *The EMBO Journal*, *25*(19), 4423-4435.

Semino, C., Angelini, G., Poggi, A., & Rubartelli, A. (2005). NK/iDC interaction results in IL-18 secretion by DCs at the synaptic cleft followed by NK cell activation and release of the DC maturation factor HMGB1. *Blood*, *106*(2), 609-616.

Sierksma, A., Lu, A., Mancuso, R., Fattorelli, N., Thrupp, N., Salta, E., Zoco, J., Blum, D., Buée, L., De Strooper, B., & Fiers, M. (2020). Novel Alzheimer risk genes determine the microglia response to amyloid-β but not to TAU pathology. *EMBO Molecular Medicine*, *12*(3), e10606. https://doi.org/10.15252/emmm.201910606

Stalder, M., Phinney, A., Probst, A., Sommer, B., Staufenbiel, M., & Jucker, M. (1999). Association of microglia with amyloid plaques in brains of APP23 transgenic mice. *The American journal of pathology*, *154*(6), 1673-1684.

Stanley, A. C., & Lacy, P. (2010). Pathways for Cytokine Secretion. *Physiology*, *25*(4), 218-229. https://doi.org/10.1152/physiol.00017.2010

Suire, C. N., Abdul-Hay, S. O., Sahara, T., Kang, D., Brizuela, M. K., Saftig, P., Dickson, D. W., Rosenberry, T. L., & Leissring, M. A. (2020). Cathepsin D regulates cerebral Aβ42/40 ratios via differential degradation of Aβ42 and Aβ40. *Alzheimer's research & therapy*, *12*(1), 80. https://doi.org/10.1186/s13195-020-00649-8

Sun, B., Zhou, Y., Halabisky, B., Lo, I., Cho, S.-H., Mueller-Steiner, S., Devidze, N., Wang, X., Grubb, A., & Gan, L. (2008). Cystatin C-cathepsin B axis regulates amyloid beta levels and associated neuronal deficits in an animal model of Alzheimer's disease. *Neuron*, *60*(2), 247-257.

Suzuki, C., Yamaguchi, J., Sanada, T., Oliva Trejo, J. A., Kakuta, S., Shibata, M., Tanida, I., & Uchiyama, Y. (2022). Lack of Cathepsin D in the central nervous system results in microglia and astrocyte activation and the accumulation of proteinopathy-related proteins. *Scientific Reports*, *12*(1), 11662. https://doi.org/10.1038/s41598-022-15805-3

Taipa, R., das Neves, S. P., Sousa, A. L., Fernandes, J., Pinto, C., Correia, A. P., Santos, E., Pinto, P. S., Carneiro, P., Costa, P., Santos, D., Alonso, I., Palha, J., Marques, F., Cavaco, S., & Sousa, N. (2019). Proinflammatory and anti-inflammatory cytokines in the CSF of patients with Alzheimer's disease and their correlation with cognitive decline. *Neurobiology of Aging*, *76*, 125-132. https://doi.org/https://doi.org/10.1016/j.neurobiolaging.2018.12.019

Thonberg, H., Chiang, H.-H., Lilius, L., Forsell, C., Lindström, A.-K., Johansson, C., Björkström, J., Thordardottir, S., Sleegers, K., Van Broeckhoven, C., Rönnbäck, A., & Graff, C. (2017). Identification and description of three families with familial Alzheimer disease that segregate variants in the SORL1 gene. *Acta neuropathologica communications*, *5*(1), 43. https://doi.org/10.1186/s40478-017-0441-9

Verheijen, J., Van den Bossche, T., van der Zee, J., Engelborghs, S., Sanchez-Valle, R., Lladó, A., Graff, C., Thonberg, H., Pastor, P., & Ortega-Cubero, S. (2016). A comprehensive study of the genetic impact of rare variants in SORL1 in European early-onset Alzheimer's disease. *Acta Neuropathologica*, *132*(2), 213-224.

Wan, L., Molloy, S. S., Thomas, L., Liu, G., Xiang, Y., Rybak, S. L., & Thomas, G. (1998). PACS-1 defines a novel gene family of cytosolic sorting proteins required for trans-Golgi network localization. *Cell*, *94*(2), 205-216.

Wang, C., Sun, B., Zhou, Y., Grubb, A., & Gan, L. (2012). Cathepsin B degrades amyloid-β in mice expressing wild-type human amyloid precursor protein. *J Biol Chem*, *287*(47), 39834-39841. https://doi.org/10.1074/jbc.M112.371641

Whyte, L. S., Fourrier, C., Hassiotis, S., Lau, A. A., Trim, P. J., Hein, L. K., Hattersley, K. J., Bensalem, J., Hopwood, J. J., Hemsley, K. M., & Sargeant, T. J. (2022). Lysosomal gene

Hexb displays haploinsufficiency in a knock-in mouse model of Alzheimer's disease. *IBRO Neurosci Rep*, *12*, 131-141. https://doi.org/10.1016/j.ibneur.2022.01.004

Willnow, T. E., & Andersen, O. M. (2013). Sorting receptor SORLA – a trafficking path to avoid Alzheimer disease. *Journal of Cell Science*, *126*(13), 2751-2760. https://doi.org/10.1242/jcs.125393

Yamazaki, H., Bujo, H., Kusunoki, J., Seimiya, K., Kanaki, T., Morisaki, N., Schneider, W. J., & Saito, Y. (1996). Elements of neural adhesion molecules and a yeast vacuolar protein sorting receptor are present in a novel mammalian low density lipoprotein receptor family member. *Journal of Biological Chemistry*, *271*(40), 24761-24768.

Zhang, Y., Sloan, S. A., Clarke, L. E., Caneda, C., Plaza, C. A., Blumenthal, P. D., Vogel, H., Steinberg, G. K., Edwards, M. S., & Li, G. (2016). Purification and characterization of progenitor and mature human astrocytes reveals transcriptional and functional differences with mouse. *Neuron*, *89*(1), 37-53.

Zhu, J., Wang, Z., Zhang, N., Ma, J., Xu, S. L., Wang, Y., Shen, Y., & Li, Y. H. (2016). Protein Interacting C-Kinase 1 Modulates Surface Expression of P2Y6 Purinoreceptor, Actin Polymerization and Phagocytosis in Microglia. *Neurochem Res*, *41*(4), 795-803. https://doi.org/10.1007/s11064-015-1754-3

Figure 1. Loss of *SORL1* results in decreased lysosomal degradation in hMGLs

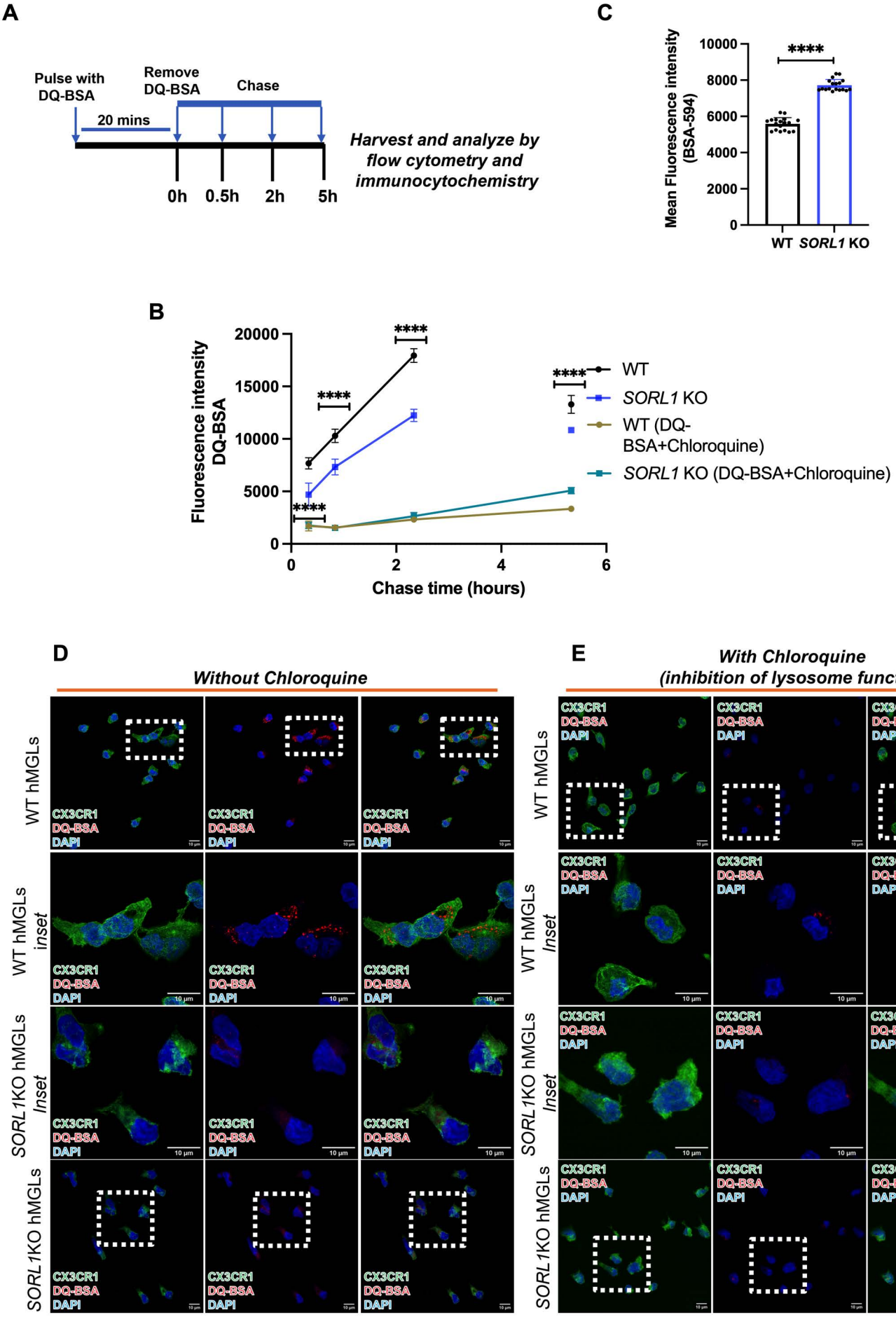

Figure 2. Loss of *SORL1* results in decreased lysosomal enzyme activity in hMGLs

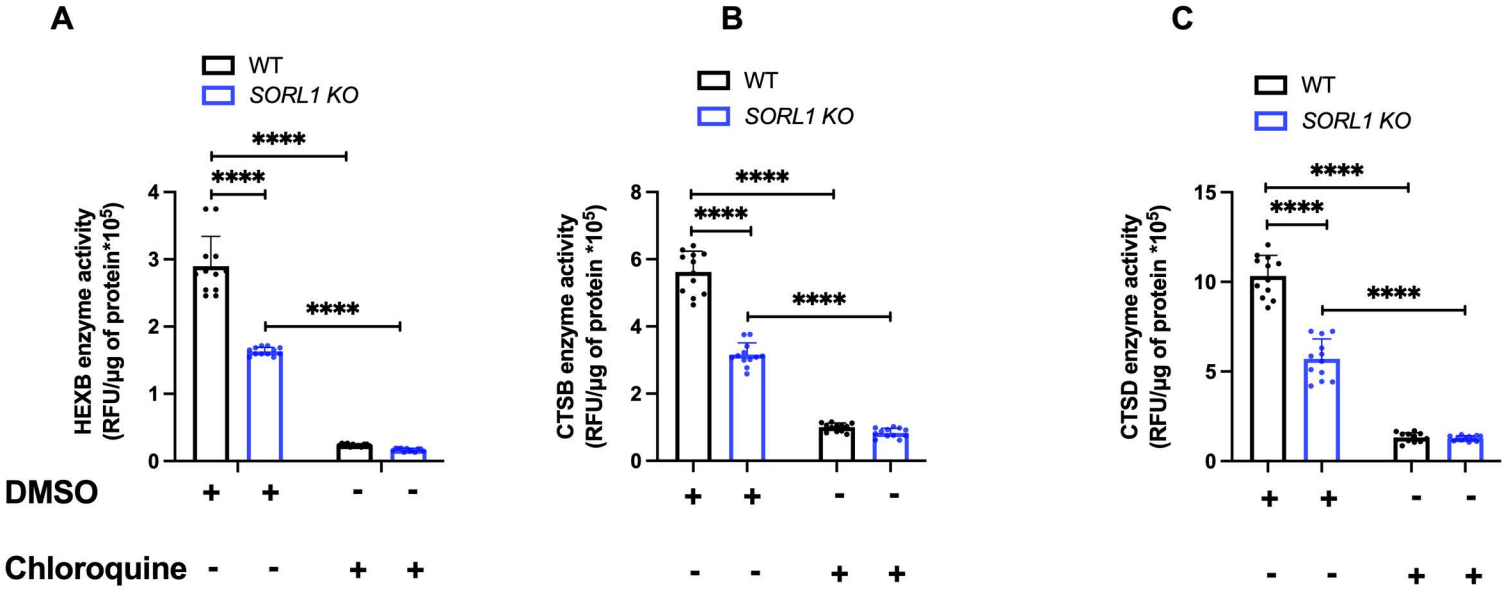

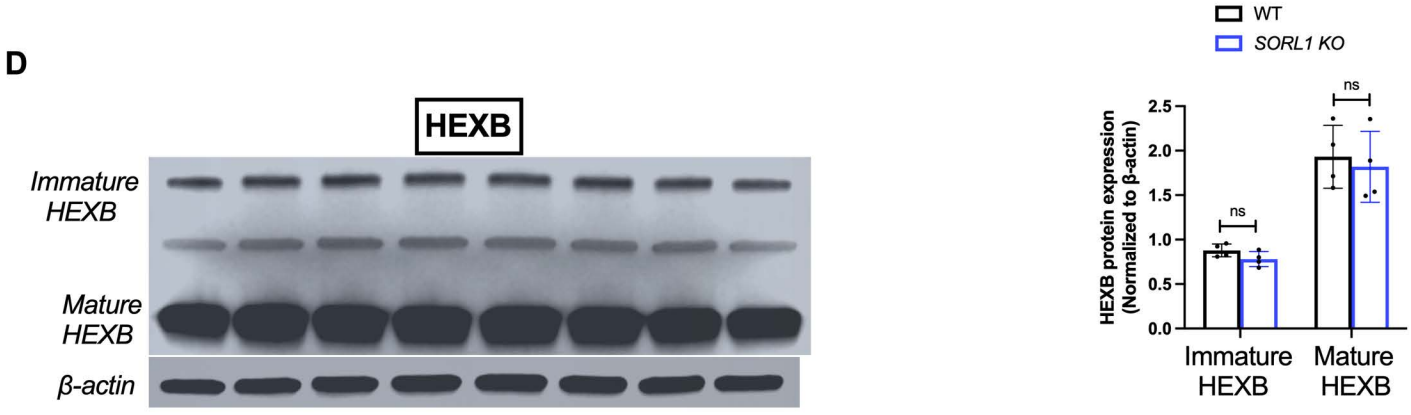

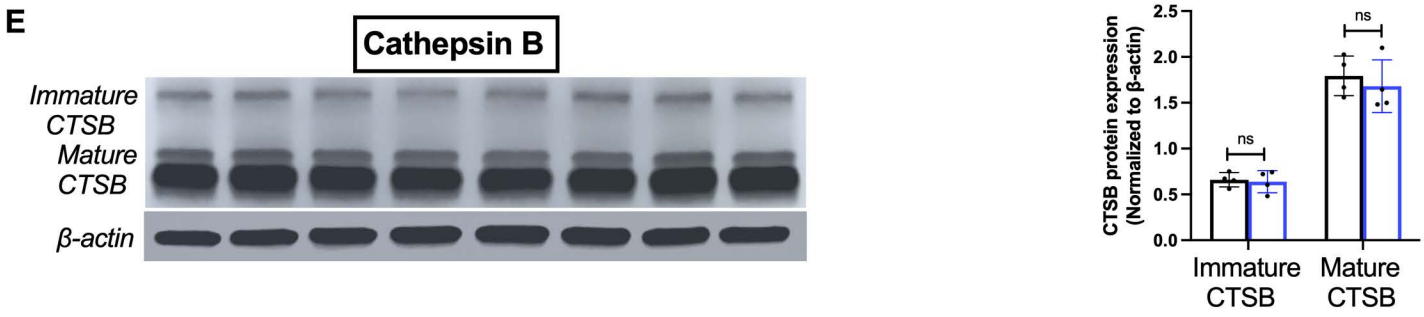

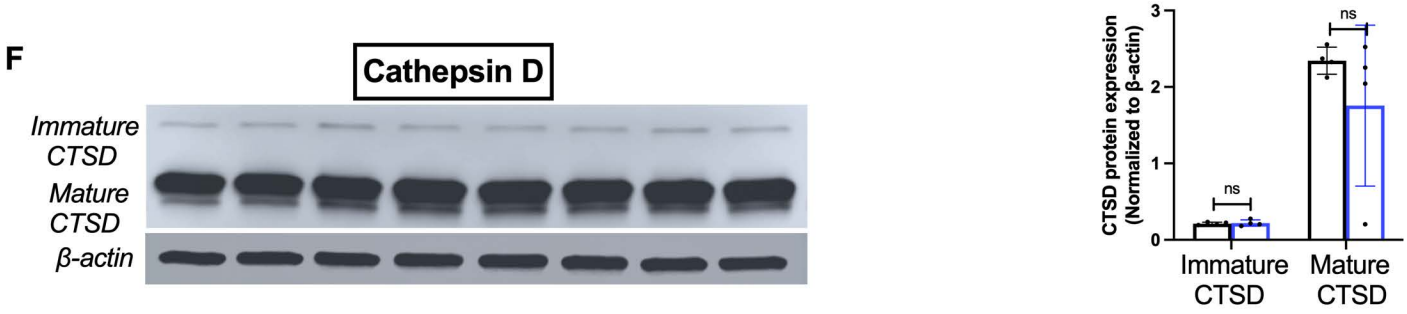

Figure 3. Loss of *SORL1* results in altered trafficking of lysosomal enzymes in hMGLs

Lysosomal enzyme colocalization with TGN38

Lysosomal enzyme colocalization with LAMP1

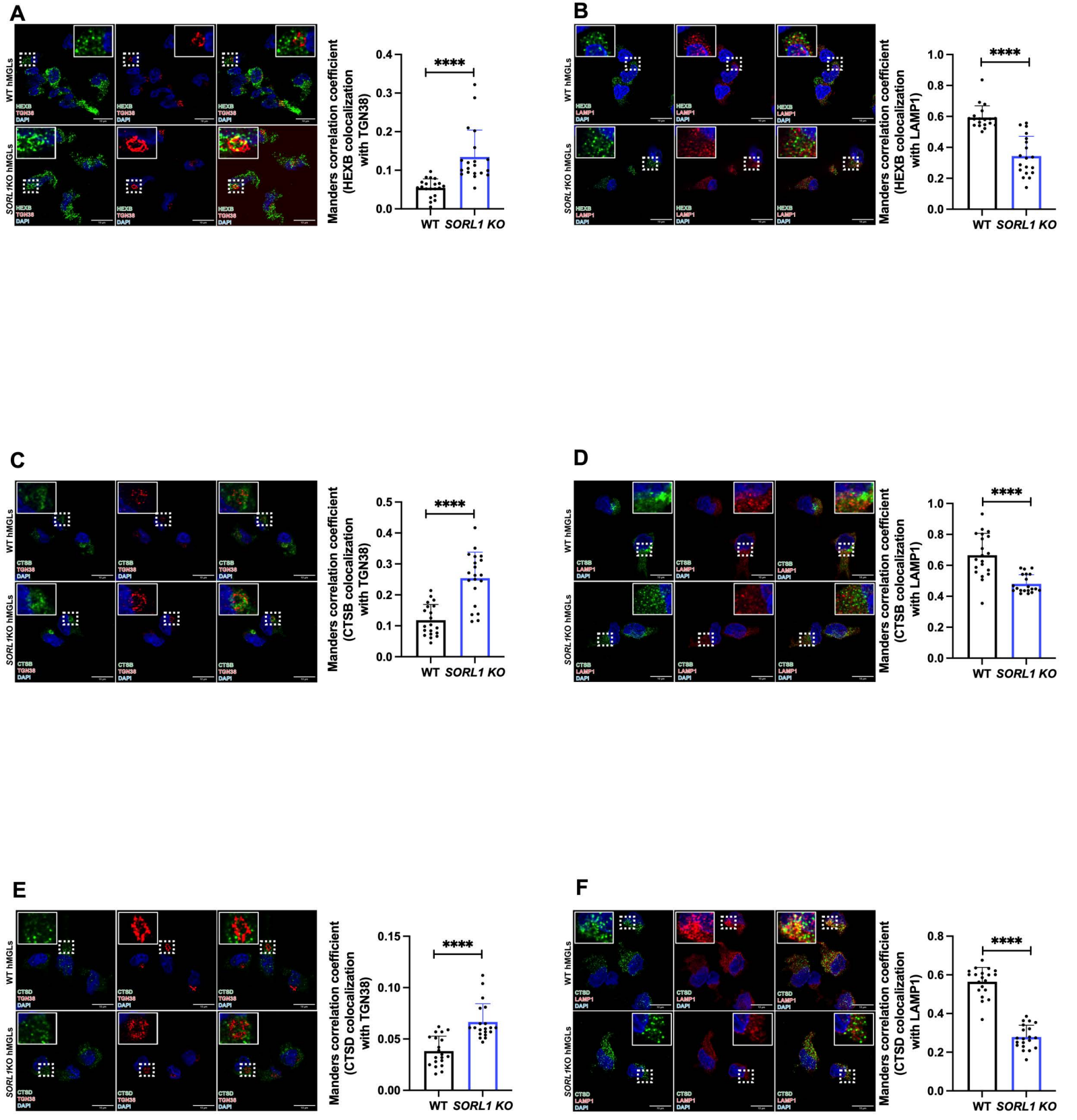

Figure 4. Loss of *SORL1* results in reduced lysosomal exocytosis in hMGLs

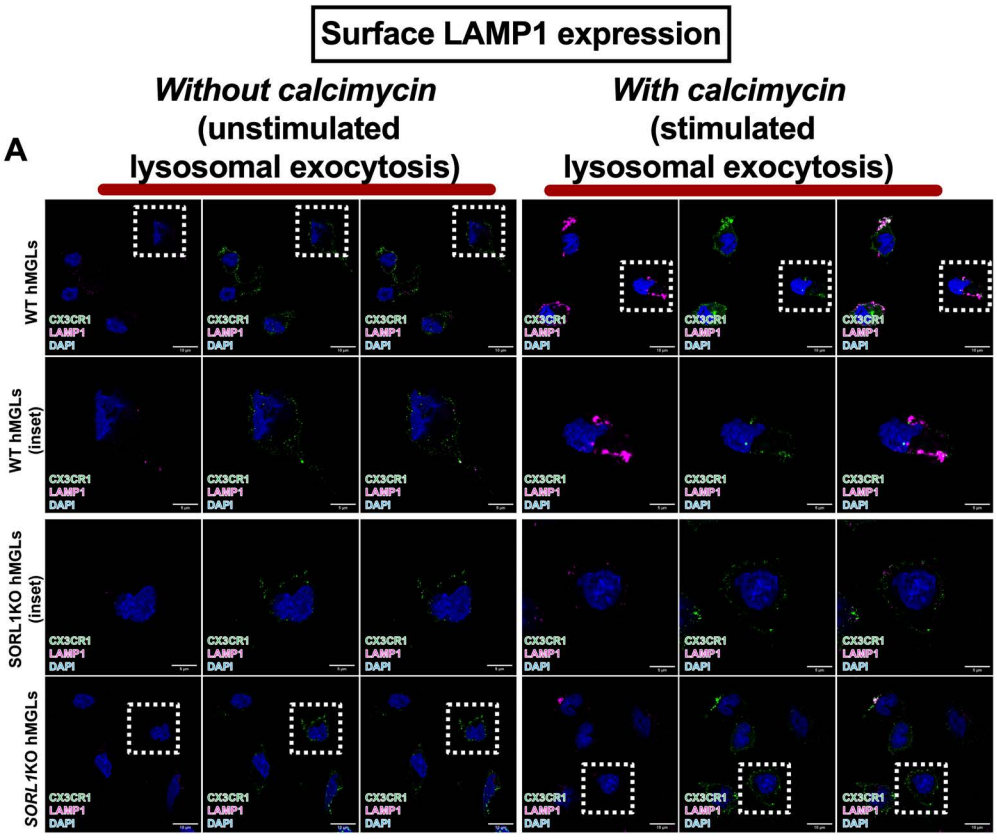

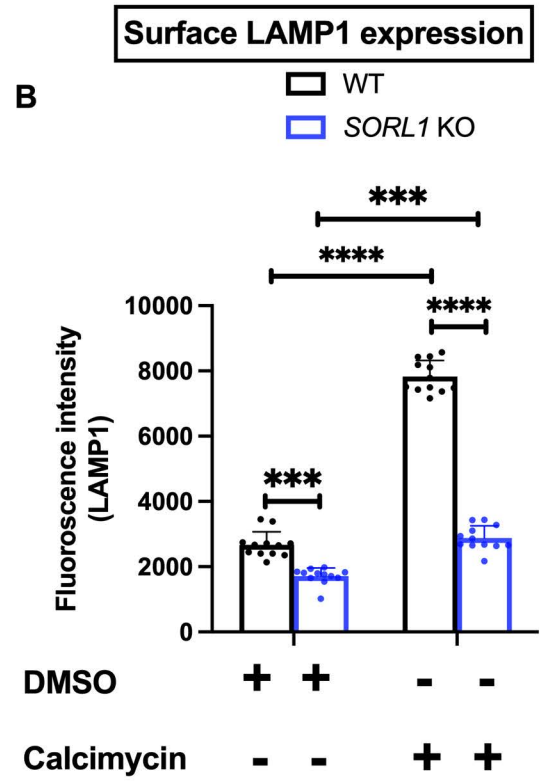

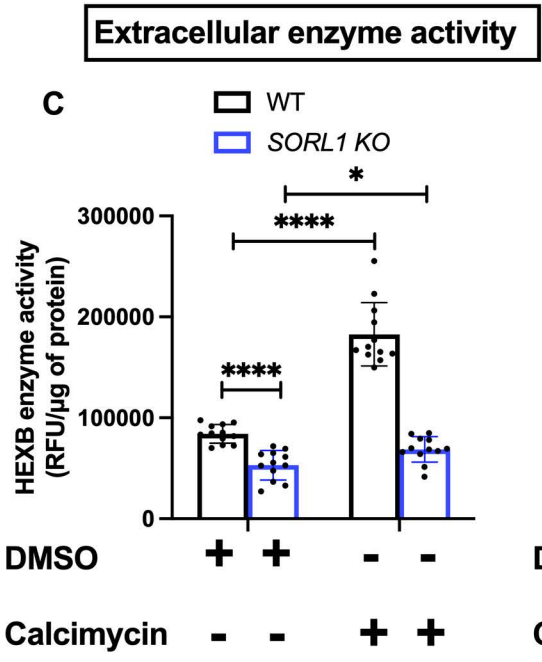

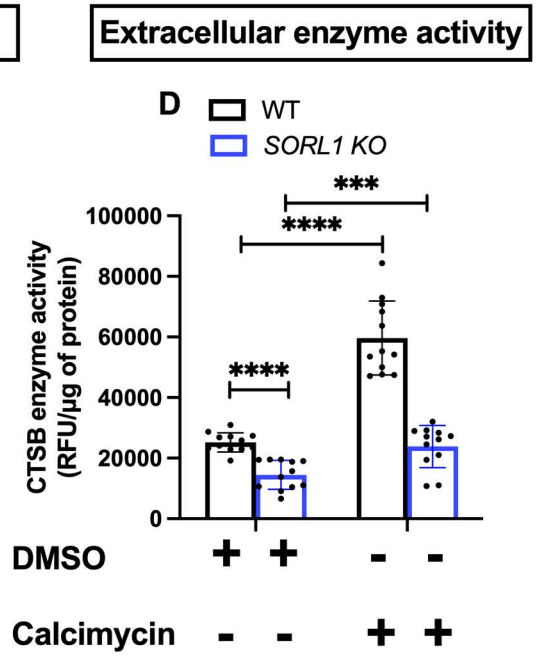

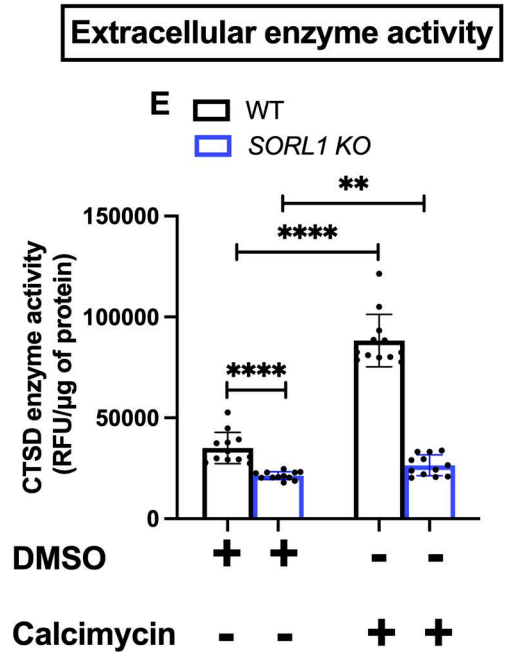

Figure 5. Loss of *SORL1* causes increased lysosomal accumulation of Aβ (1-42) and synaptosomes in hMGLs

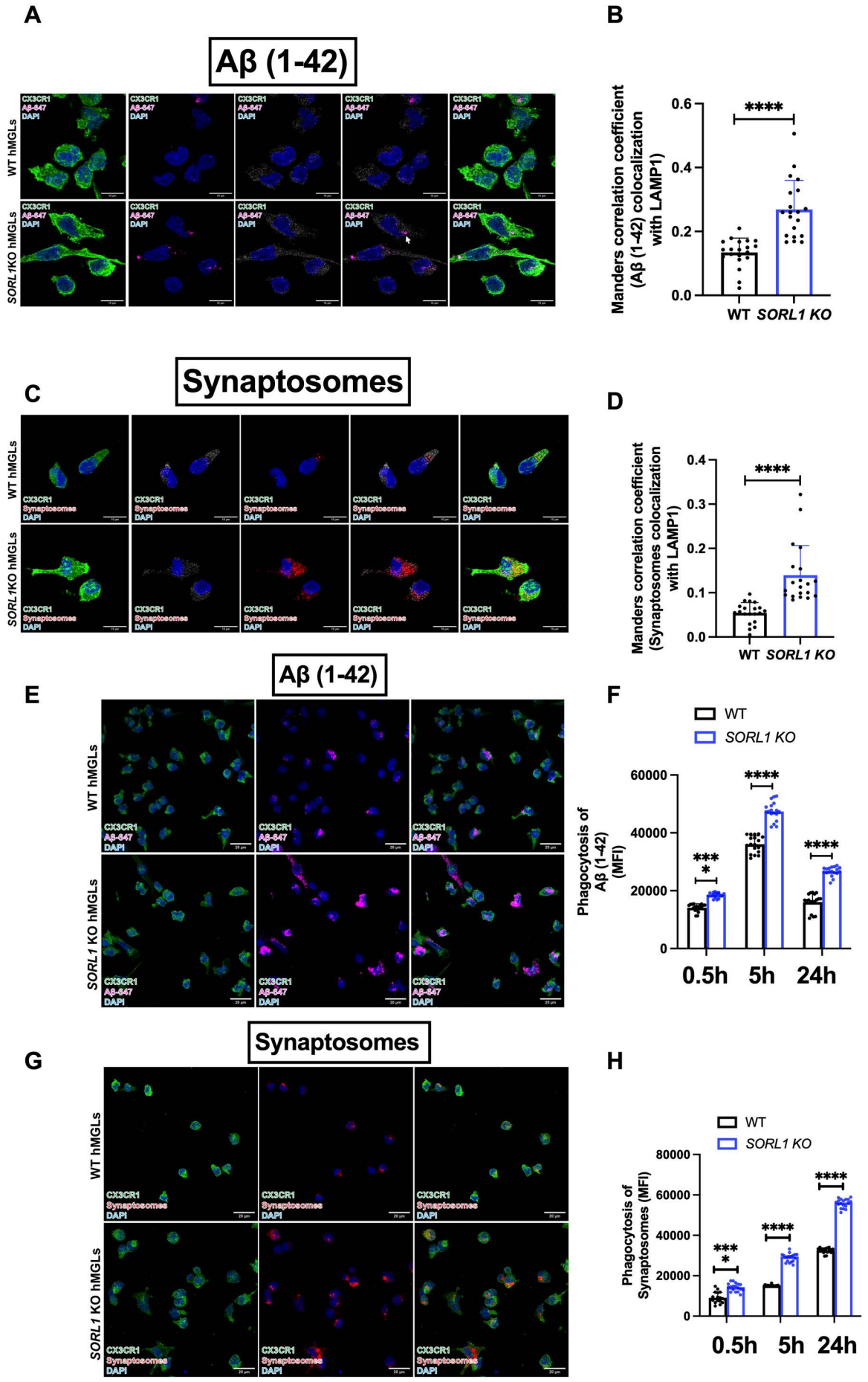

Figure 6. Loss of *SORL1* results in reduced inflammatory response to pro-inflammatory stimuli in hMGLs

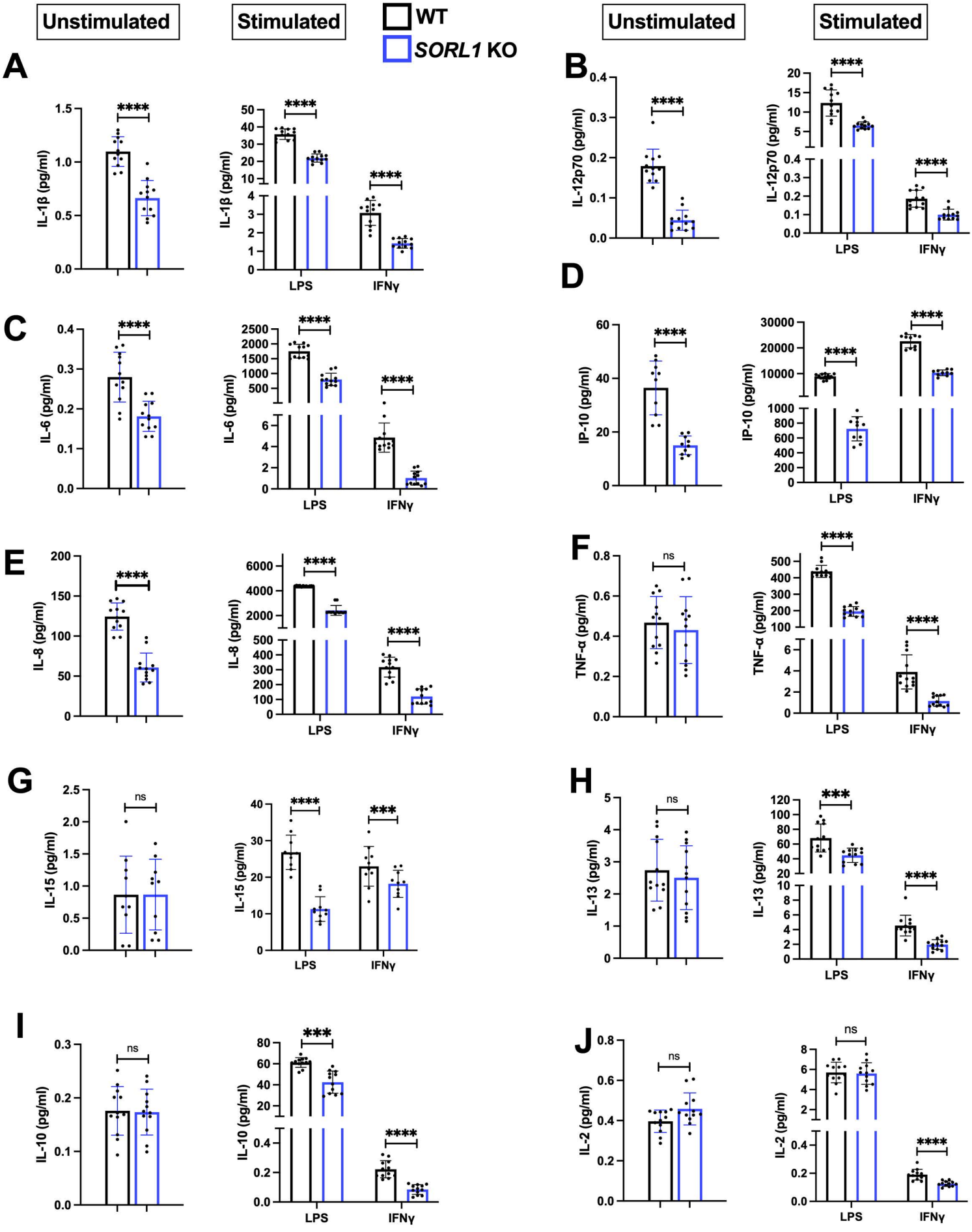

Figure 7. Working model

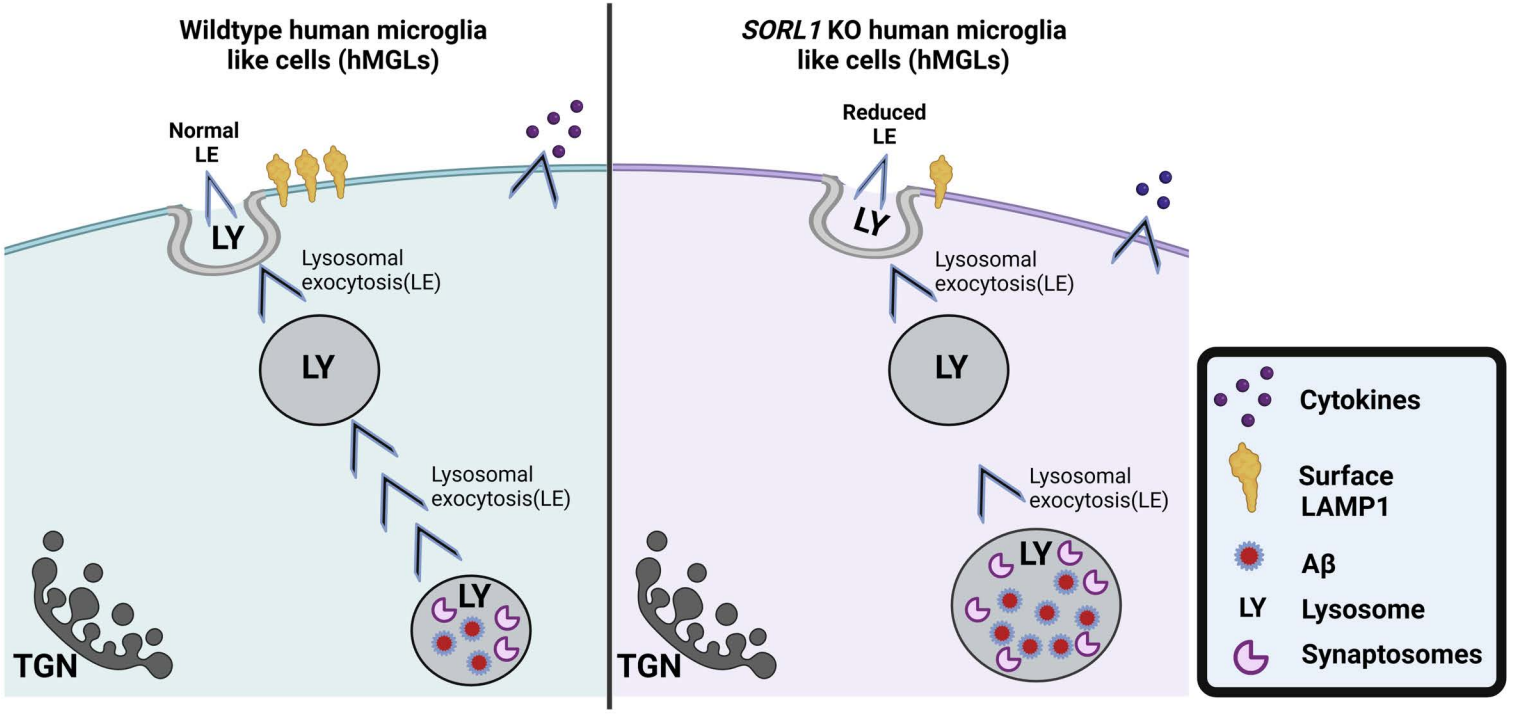

Supplementary Figure 1. Loss of *SORL1* does not alter differentiation of iPSCs into HPCs and hMGLs

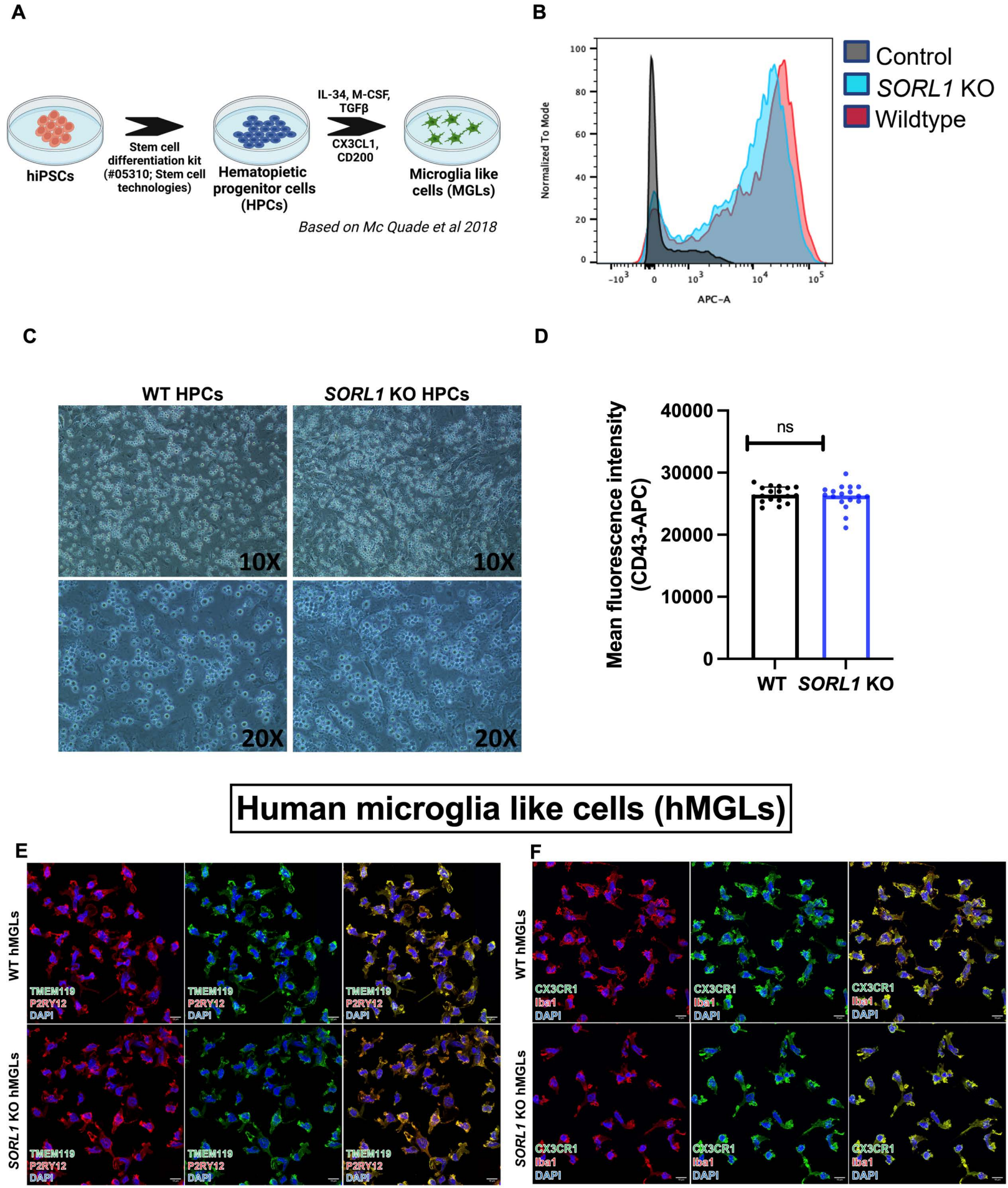

Supplementary Figure 2. Loss of *SORL1* results in decreased enzymes activity of iMGLs

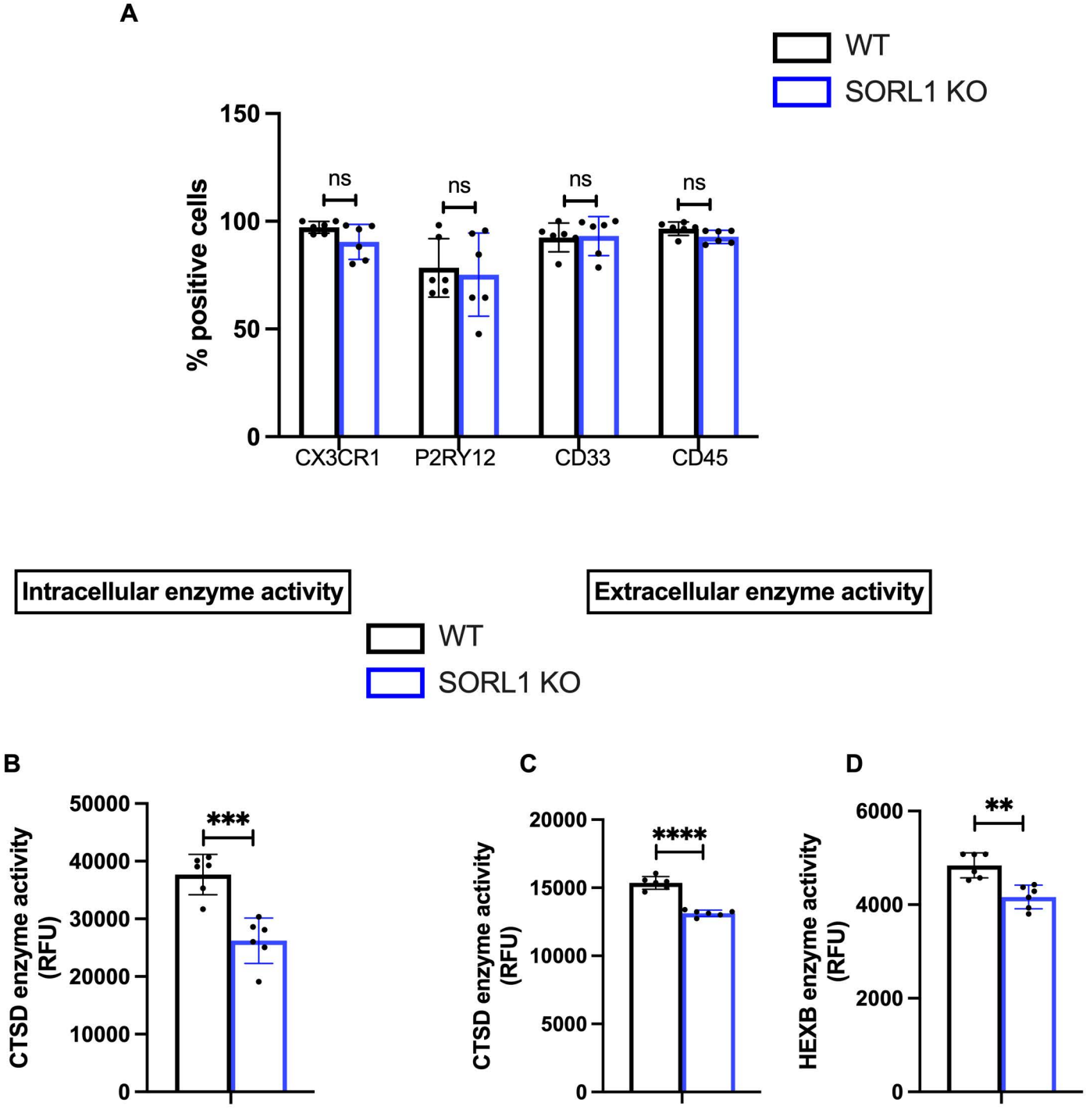

Supplementary Figure 3. Loss of *SORL1* results decreased intensity of Phrodo dye conjugated with fibrillar Aβ 1-42 in *SORL1*KO hMGLs

A

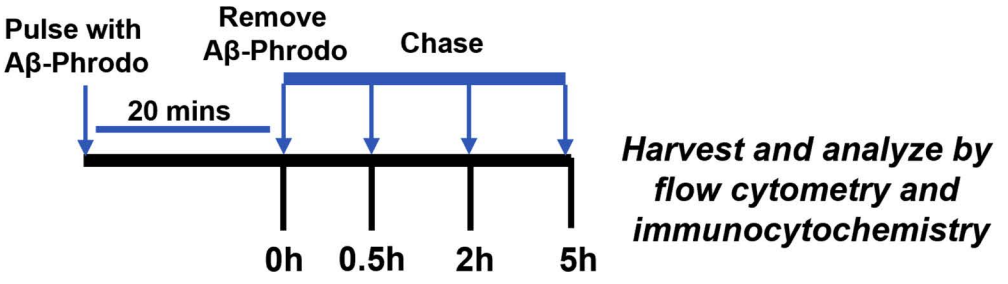
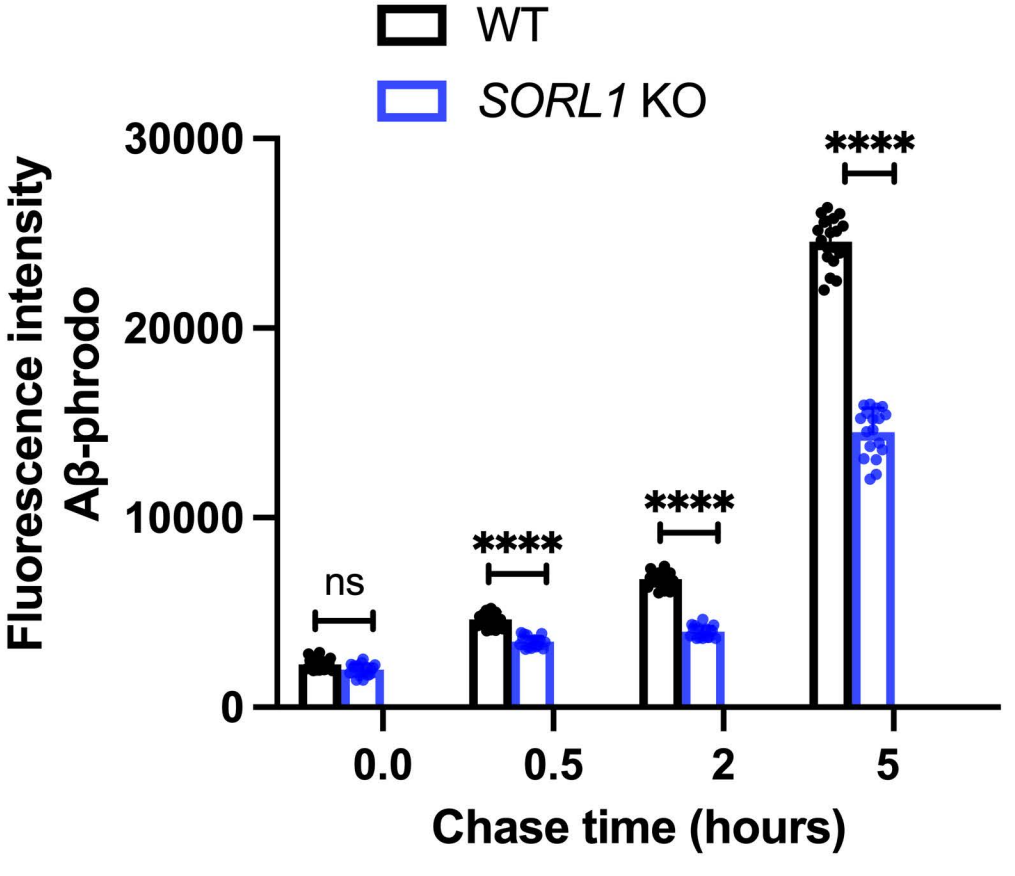
B